HHS Public Access

Author manuscript

J Thromb Haemost. Author manuscript; available in PMC 2025 September 01.

Published in final edited form as:

J Thromb Haemost. 2024 September ; 22(9): 2514–2530. doi:10.1016/j.jtha.2024.05.019.

Extracellular histones: a unifying mechanism driving platelet-dependent extracellular vesicle release and thrombus formation in COVID-19

Alicia S. Eustes[1], **Azaj Ahmed**[1], **Jagadish Swamy**[1], **Gokul Patil**[1], **Melissa Jensen**[1], **Katina M. Wilson**[1], **Shibani Kudchadkar**[1], **Abdul Wahab**[1], **Usha Perepu**[1], **Francis J. Miller Jr.**[2], **Steven R. Lentz**[1], **Sanjana Dayal**[1,3]

[1]Department of Internal Medicine, University of Iowa, Iowa City, IA, USA

[2]Department of Internal Medicine, Vanderbilt University Medical Center and VA Medical Center, Nashville, TN, USA

[3]Iowa City VA Healthcare System, USA

Abstract

Background: COVID-19 can cause profound inflammation and coagulopathy, and while many mechanisms have been proposed, there is no known common pathway leading to a prothrombotic state.

Objectives: From the beginning of the COVID-19 pandemic, elevated levels of extracellular histones have been found in plasma of patients infected with SARS-CoV-2. We hypothesized that platelet activation triggered by extracellular histones might represent a unifying mechanism leading to increased thrombin generation and thrombosis.

Methods: We utilized blood samples collected from an early clinical trial of hospitalized COVID-19 patients (NCT04360824) and recruited healthy subjects as controls. Using plasma samples, we measured the procoagulant and prothrombotic potential of circulating extracellular histones and extracellular vesicles (EVs). Platelet prothrombotic activity was assessed via thrombin generation potential and platelet thrombus growth. Circulating EVs were assessed for

Corresponding Author: Sanjana Dayal, PhD, FAHA, Associate Professor, Department of Internal Medicine, The University of Iowa Carver College of Medicine, Section of Hematology, 25 S Grand Ave., Iowa City, IA 52246, Fax: 319-353-8383, sanjana-dayal@uiowa.edu.

Authorship contributions

A.S. Eustes designed and conducted the experiments, interpreted the results and helped write the manuscript. A. Ahmed conducted assays related to flowcytometry, and EVs measurements. J. Swamy assisted with sample collection, processing, and in conducting some assays. G. Patil assisted with flowcytometry and performed protein estimation in EVs. M. Jensen and K.M. Wilson assisted with sample collection and processing. A. Wahab, S. Kudchadkar, and U. Perepu assisted with recruitment of patient or controls. F.J. Miller provided a critical reagent. S.R. Lentz helped with patient recruitment and participated in designing experiments, data interpretation and helped write the manuscript. S. Dayal conceived the idea, directed the project, designed the experiments, interpreted the results, and helped write the manuscript. All authors assisted with the preparation and editing of the manuscript.

Disclosure of Conflict of Interest

We have nothing to disclose.

thrombin generation potential *in vitro* in plasma and enhancement of thrombotic susceptibility *in vivo* in mice.

Results and Conclusions: Compared to controls, COVID-19 patients had elevated plasma levels of citrullinated histone H3, cell free DNA, nucleosomes, and EVs. Plasma from COVID-19 patients promoted platelet activation, platelet-dependent thrombin generation, thrombus growth under venous shear stress, and release of platelet-derived EVs. These prothrombotic effects of COVID-19 plasma were inhibited by an RNA aptamer that neutralizes both free and DNA-bound histones. EVs isolated from COVID-19 plasma enhanced thrombin generation *in vitro* and potentiated venous thrombosis in mice *in vivo.* We conclude that extracellular histones and procoagulant EVs drive the prothrombotic state in COVID-19 and that histone-targeted therapy may prove beneficial.

Keywords

COVID-19; extracellular vesicles; histones; thrombin generation; thrombosis

Introduction

Coronavirus disease 2019 (COVID-19) is a thrombo-inflammatory state. In severe cases, it leads to profound inflammation and coagulopathy with progression to multiple organ failure [1–4]. Venous thromboembolism occurs in 12 to 28% of hospitalized COVID-19 patients despite pharmacological thromboprophylaxis [5–8]. Many potential mediators of thrombosis in COVID-19 have been proposed; however, no unifying mechanism has been established. The identification of a common pathway leading to thrombosis in COVID-19 could establish new biomarkers for thrombotic risk stratification and direct the development of antithrombotic therapeutics toward novel drug targets.

Proposed mediators of thrombosis in COVID-19 include endotheliopathy [9, 10], platelet activation [9, 11, 12], cytokine storm [13–17], neutrophil activation [18–22], complement activation [18] and antiphospholipid antibodies [21]. All of these processes can induce cell death pathways such as apoptosis, necrosis, or extracellular trap (ET) formation via direct or indirect mechanisms [23–27], resulting in elevation of extracellular histones [23, 28–31].

Many patients with COVID-19 have elevated plasma levels of free histones such as citrullinated histone H3 (H3Cit) as well as DNA-bound histones such as nucleosomes [14, 20, 22, 32–35]. Interestingly, elevated plasma levels of H3Cit in COVID-19 are positively associated with disease severity and may serve as a prognostic marker of thrombosis [22, 33–35]. In COVID-19, H3Cit is not only elevated in blood plasma but also in lung tissue [19, 36], bronchoalveolar fluid [33], and tracheal aspirates [14, 36], suggesting that histones may be not only a marker but also a potential mediator of pulmonary or cardiac thrombosis. Notably, elevation of extracellular histones has been a persistent feature of COVID-19 throughout the pandemic [37], indicating that it is an assiduous characteristic of SARS-CoV-2 and its variants and subvariants.

In mice, administration of exogenous histones at high concentrations causes lethality [38]. At sub-lethal doses, histones promote acute inflammation [39] and thrombosis by

affecting both procoagulant and anticoagulant pathways [40–43]. Elevated plasma levels of extracellular histones have been reported in thrombotic conditions such as myocardial infarction [44], stroke [45, 46], ischemic outcomes after angioplasty [47], deep vein thrombosis [48], and disseminated intravascular coagulation [43]. Extracellular histones have the potential to activate platelets via toll-like receptors TLR2 and TLR4, leading to histone-mediated platelet activation and enhanced thrombin generation [49, 50]. Thrombin generation potential is enhanced in COVID-19 [9, 51–54], but the potential role of extracellular histones and the downstream mechanisms of thrombin generation and thrombus formation have not been delineated.

Using plasma samples from an early clinical trial of hospitalized COVID-19 patients [55], we investigated the mechanistic role of extracellular histones in inducing platelet prothrombotic activity, release of procoagulant extracellular vesicles (EVs), thrombin generation, and thrombus formation in COVID-19. We also investigated the prothrombotic potential of EVs isolated from COVID-19 plasma to augment venous thrombosis in a mouse model.

Methods

Human subjects

Blood samples were collected from hospitalized adult patients with COVID-19 from April 2020 to January 2021 as part of an investigator-initiated, open-label randomized controlled trial (NCT04360824) [55]. Infection with SARS-CoV-2 was confirmed by nasopharyngeal swab polymerase chain reaction. Patients were eligible if they were admitted to an intensive care unit (ICU) and/or had coagulopathy defined as a modified International Society on Thrombosis and Haemostasis Overt DIC score ≥ 3 [55]. Control blood samples were collected from healthy subjects who were free of cardiovascular and metabolic disease and were not taking any medications. Written informed consent was obtained from all controls and patients or their legally authorized representatives. All protocols were approved by the institutional review board of the University of Iowa.

Mice

All animal studies were approved by the institutional animal care and use committees at the University of Iowa. C57BL6J mice were obtained from the Jackson Laboratory and were bred and maintained in the animal facility at the University of Iowa. Both male and female mice were included in the study design.

Blood sample processing

Blood was collected in tubes containing 3.2% sodium citrate. 50 μg/mL corn trypsin inhibitor (CTI, Haematologic Technologies) was added to some of the samples within 60 minutes of collection and before processing to prevent contact-dependent coagulation. Blood was centrifuged at 1000 *g* for 10 minutes at room temperature to collect platelet poor plasma (PPP), which was centrifuged further at 10,000 *g* for 10 minutes to obtain platelet free plasma (PFP). For some experiments, EVs were isolated from PFP by centrifugation at 20,000 *g* for 30 minutes followed by a wash in PBS and a second spin at 20,000 *g* for

30 minutes [56]. The resultant EV-free plasma was stored for use in other experiments. The isolated EVs were characterized by transmission electron microscopy, nanoparticle tracking analysis, western blotting, and flow cytometry or used in thrombin generation or experimental venous thrombosis. See details of EV isolation and characterization in Supplemental Data.

Platelets were isolated from whole blood using density centrifugation as described previously [57] (see Supplemental Data for details). Isolated platelets were suspended in Tyrode's buffer at pH 7.35 containing 0.35% bovine serum albumin or in PPP or EV-free PFP as needed. For some experiments, after incubation platelets were pelleted and resuspended in pooled healthy PFP containing CTI or in the Tyrode buffer. In other experiments, PPP was pre-treated for 5 minutes with 1 μM of histone binding aptamer-7 (HBA7; previously referred to as KU7) [58] or with 250 ng/mL of anti-TLR2 prior to incubation with platelets.

Thrombin generation

Thrombin generation in PFP was measured using the Calibrated Automated Thrombogram (Diagnostica Stago, Inc) [59]. PFP from patients or controls was pre-treated with heparinase (>125 IU/mL) (Hepzyme, Seimens) to inactivate any residual heparin or low-molecular weight heparin in the plasma. PFP (80 μl) was incubated with 20 μl of "trigger" (either 1 pM tissue factor (TF), 4 μM phospholipids, or both) in round-bottom 96-well Immulon plates for 10 minutes at 37° C before a FluCa fluorogenic substrate (Z-GGR-AMC) buffer solution containing $CaCl_2$ was added and generation of thrombin was monitored for 60 minutes [60]. These assays were conducted either in the presence or absence of platelets (5×10^8 cells/mL), or with the addition of exogenous EVs, DNase 1 (20 units/mL, Worthington 65006344) or heat-inactivated DNase 1, histone H3.1 (500–25,000 ng/mL, designated as histone H3, New England Biolabs M2503S), H3Cit (500–25,000 ng/mL, Cayman Chemicals 17926), or nucleosomes (500–10,000 ng/mL, EMD Millipore 14–1057). Peak thrombin (nM), velocity index (nM/min), lag time (min), time to peak (Tmax) (min), and endogenous thrombin potential (ETP) (nM.min) were determined using Thrombinoscope software 5.0.

Platelet-derived EV production

To generate platelet-derived EVs (PEVs), platelets from healthy subjects were stimulated with either EV-free plasma or agonists in Tyrode's buffer containing 2 mM $CaCl_2$ [convulxin (Santa Cruz) plus thrombin (Chronolog), histone H3.1 (designated as histone H3 or H3), H3Cit, or nucleosomes] for 1 hour at 37° C. In some experiments, histone H3, H3Cit, and nucleosomes were pre-incubated either with 1 μM HBA7 for 5 minutes or platelets were pre-incubated with anti-TLR2, anti-TLR4, or IgG (Invitrogen 16-9922-82, 16-9917-82, 16-4724-82 respectively) for 15 minutes at room temperature. Platelets were then pelleted by centrifugation at 1,000 *g* for 8 minutes and the EVs were isolated as detailed in Supplemental Data.

Experimental venous thrombosis

Experimental venous thrombosis was performed using the stenosis model of inferior vena cava (IVC) ligation in 8–12 week old male C57BL6/J mice (Jackson Laboratory) in which

the IVC was partially ligated just below the left renal vein using a 6.0 silk suture [21]. Side branches were not ligated. Immediately after the IVC ligation, EVs isolated from 500 μl of either COVID-19 or control PFP were injected retro-orbitally. After 48 hours, the thrombus that formed inferior to the ligation was harvested and the length and weight of the thrombus were recorded.

Statistical analysis

All data were analyzed using GraphPad Prism 9. Histograms of all measures were examined to graphically assess normality.[61] For data in a normal distribution, the unpaired t-test was used for two-group comparisons and the one-way ANOVA was used for multiple groups followed by Dunn's test for comparison. For data not in a normal distribution, the Mann-Whitney test was used for two-group comparisons and the Kruskal-Wallis test used for multiple groups. For paired samples, the paired t-test was used for data in a normal distribution and the Wilcoxon matched pairs signed rank test used for data not in a normal distribution. Repeated measures data were analyzed using a mixed effects ANOVA. Spearman's rank-based correlation was performed to assess the relationships between continuous measures for overall or cohort-stratified samples.

Data sharing statement

Data are available from the corresponding author upon request.

Results

Plasma from COVID-19 patients enhances platelet-dependent thrombin generation and thrombus formation *in vitro*

Plasma samples were collected from 103 hospitalized COVID-19 patients and 68 healthy subjects (controls). Baseline characteristics of the patients and controls are summarized in Table 1. The median age of the COVID-19 patients was 63 years, 53% were male, 66% were admitted to an intensive care unit (ICU), and their hemostatic parameters were notable for elevated D-dimer (median 1.5 μg/mL, IQR 0.8–3.9 μg/mL). The 30-day mortality was 17.5% and 14% suffered from venous or arterial thrombosis. Full details of the clinical course of the patients were reported in the primary clinical trial publication [55].

To determine if COVID-19 plasma promotes platelet activation, platelets isolated from healthy subjects were incubated for 15 minutes in PPP prepared from either COVID-19 or healthy controls. Flow cytometry was performed to measure platelet surface $\alpha_{II}b\beta3$ activation by PAC1 binding and phosphatidylserine (PS) exposure by annexin V binding. We observed that platelets incubated with COVID-19 plasma demonstrated activation of $\alpha_{II}b\beta3$ ($p < 0.01$) and increased PS exposure ($p < 0.001$) compared to control plasma (Figure 1 A–B).

To determine if COVID-19 plasma promotes platelet-dependent thrombin generation, platelets isolated from healthy subjects were incubated with PPP from either controls or COVID-19 patients, pelleted, and resuspended in pooled healthy PFP containing CTI to inhibit contact activation. Thrombin generation was triggered with TF without exogenous

phospholipids. Compared to pooled healthy PFP without added platelets, the addition of platelets enhanced peak thrombin generation (Figure 1 C). This effect was greater in platelets incubated with COVID-19 plasma compared to platelets incubated with control plasma ($p < 0.01$). Platelets incubated with COVID-19 plasma also demonstrated greater enhancement of velocity index and ETP compared to platelets incubated with control plasma ($p < 0.01$ for both). No associations were observed between thrombin generation and age, body mass index (BMI), or sex of the COVID-19 patients (Figure S1 A–O).

We next determined the effect of COVID-19 PPP on platelet thrombus formation on a collagen matrix under venous shear stress in a microfluidic flow chamber *in vitro*. Platelets from healthy subjects were resuspended in recalcified PPP from either controls or COVID-19 patients for 15 minutes and then perfused over collagen (Figure 1 D). We observed a more rapid accumulation of platelets incubated with COVID-19 PPP compared to control PPP, and significantly larger platelet thrombi developed after 10 minutes with COVID-19 PPP compared to control PPP ($p < 0.05$) (Figure 1 E). Platelet accumulation was not associated with age, BMI, nor sex of the COVID-19 patients (Figure S1 P–R).

Plasma from COVID-19 patients promotes production of platelet-derived extracellular vesicles

To further determine the effect of COVID-19 plasma on platelets, we measured the production of PEVs, which have been demonstrated to promote thrombin generation [62, 63] and have been found in the plasma of COVID-19 patients [9, 64–70]. When platelets from healthy control subjects were incubated with EV-free plasma from either controls or COVID-19 patients for one hour, we observed that EV-free plasma from COVID-19 patients, but not controls, triggered platelets to produce annexin V/CD41-double positive PEVs as analyzed by flow cytometry (Figure 1 F). Neither age, BMI, nor sex was associated with PEV production (Figure S1 S–U).

To determine if PEVs enhance thrombin generation, the isolated PEVs were added to pooled control EV-free PFP containing CTI. Thrombin generation was once again triggered with TF without exogenous phospholipids. The addition of PEVs isolated from platelets stimulated with COVID-19 EV-free plasma increased the peak thrombin and velocity index significantly compared to PEVs produced from platelets stimulated with control EV-free plasma ($p < 0.02$ and 0.01) (Figure 1 G).

Extracellular histones in COVID-19 plasma mediate platelet-dependent thrombin generation, *in vitro* thrombus formation, and PEV production

One of the hallmarks of SARS-CoV-2 infection is the increased presence of markers of cell death, including extracellular histones, in plasma [14, 20, 22, 32–35]. Consistent with these reports, we observed that levels of cell-free DNA (cfDNA), H3Cit, and nucleosomes were significantly higher in the plasma of COVID-19 patients than in controls (Figure S2 A–C). Among the COVID-19 patients, levels of cfDNA, H3Cit, and nucleosomes were higher in patients who suffered 30-day mortality compared to survivors (Figure S2 D–F). Levels of cfDNA, H3Cit, and nucleosomes did not differ significantly between COVID-19 patients who were or were not admitted to an ICU (Figure S2 G–I) or between those who did or did

not have a bleeding event (Figure S2 J–L). Levels of nucleosomes but not cfDNA or H3Cit were significantly higher in patients who experienced a thrombotic event (Figure S2 M–O).

Extracellular histones can activate platelets resulting in increased thrombin generation [50]. Intriguingly, we observed that when added to control PRP containing CTI, histone H3 increased peak thrombin generation and velocity index in a dose dependent fashion (Figure S3 A). Similar dose-dependent increases in thrombin generation were observed with H3Cit and nucleosomes (Figure S3 B–C). Compared to histone H3, H3Cit increased peak thrombin to a similar degree while nucleosomes increased peak thrombin to a greater degree (Figure S3 D). This response was dependent on platelets, since in the absence of platelets neither histone H3, H3Cit, nor nucleosomes altered thrombin generation (Figure S3 E).

To determine if extracellular histones in COVID-19 plasma mediated the enhanced platelet-dependent thrombin generation seen in Figure 1, plasma from COVID-19 patients or controls was pretreated with either vehicle or HBA7, an RNA aptamer that binds and neutralizes histones [58]. We observed that HBA7 significantly attenuated the platelet-dependent increase in thrombin generation mediated by platelets that were incubated with COVID-19 plasma ($p < 0.01$) but not with control plasma (Figure 2 A). In a control experiment, HBA7 did not affect thrombin generation in control or COVID-19 PFP without added platelets (Figure S4), confirming that the histone-mediated effects on thrombin generation are platelet dependent. HBA7 also inhibited *in vitro* platelet thrombus formation with COVID-19 plasma-treated platelets ($p < 0.005$) with near normalization of platelet accumulation to that observed with platelets treated with control plasma (Figure 2 B–C).

Further, the HBA7 aptamer prevented the COVID-19 plasma-mediated production of annexin V/CD41 double positive PEVs as measured by flow cytometry ($p < 0.0001$) (Figure 3 A). This effect of the aptamer resulted in a decrease in peak thrombin and velocity index when PEVs from platelets stimulated with COVID-19 plasma were added to control EV-free PFP ($p < 0.05$) (Figure 3 B). The levels of PEVs generated from platelets stimulated with COVID-19 EV-free plasma correlated positively with the concentrations of H3Cit and nucleosomes in the patient plasmas (Figure 3 C–D). Together, these data indicate that histones in COVID-19 plasma generate procoagulant platelets and PEVs and facilitate the formation and growth of platelet thrombi on collagen under shear stress.

Extracellular histones promote the production of PEVs via TLR2

Given our novel observation that histones in COVID-19 plasma can activate platelets to release PEVs, we sought to determine the relative potential of different forms of extracellular histones (histone H3, H3Cit, and nucleosomes) to produce PEVs. We incubated washed platelets from control subjects suspended in Tyrode's buffer with recombinant histone H3, recombinant citrullinated H3, or nucleosomes, and annexin V/CD41-double positive EVs were quantitated by flow cytometry. We found that histone H3 stimulated the production of PEVs with a biphasic dose response, thresholding at 250 ng/mL and declining at 500 ng/mL (Figure 4 A). In contrast, both H3Cit and nucleosomes stimulated PEV production with a relatively linear dose dependency. The levels of PEVs generated with all three forms of histones exceed that of platelets stimulated with convulxin and thrombin.

The addition of HBA7 significantly decreased PEV generation by histone H3, H3Cit, and nucleosomes (Figure 4 B–D).

Since extracellular histones can activate platelets via toll-like receptors TLR2 and TLR4 [49, 50, 71], we used neutralizing antibodies to determine whether histones stimulate the production of PEVs through these receptors. We found that pre-incubation with a TLR2 neutralizing antibody significantly decreased PEV production from platelets stimulated with histone H3 or H3Cit, but not nucleosomes (Figure 4 E–G). Pre-incubation with a TLR4 blocking antibody did not significantly inhibit PEV production stimulated by H3, CitH3, or nucleosomes.

We next tested whether the enhanced PS exposure and integrin activation observed when control platelets are incubated in COVID-19 plasma is also mediated via histones in a TLR2-dependent manner. Washed platelets from healthy subjects were resuspended in either COVID-19 or control plasma. Plasma was either untreated or treated with HBA7 or anti-TLR2 prior to suspending platelets. Flow cytometry was performed to measure platelet surface PS exposure by annexin V binding and αIIbβ3 activation by PAC1 binding. The procoagulant effects of COVID-19 plasma on PS exposure and αIIbβ3 activation were inhibited by incubation with either HBA7 ($p < 0.01$ for annexin V and $p < 0.05$ for PAC-1) or anti-TLR2 ($p < 0.05$ for both annexin V and PAC-1) (Figure 5 A–B). These findings provide further evidence that extracellular histones in COVID-19 plasma promote prothrombotic platelet activation via TLR2.

Extracellular vesicles present in COVID-19 plasma accentuate thrombin generation potential

Having demonstrated that PEVs produced from platelets activated with histones in COVID-19 plasma can enhance thrombin generation, we next sought to examine the effect of endogenous EVs isolated from COVID-19 plasma itself. EVs were isolated from control or COVID-19 PFP via ultracentrifugation and analyzed by transmission electron microscopy (Figure S5 A). Isolated EVs ranged in diameter from less than 50 nm to up to 200 nm (Figure S5 B). There was a non-significant elevation in the number of EVs isolated from COVID-19 patients compared to controls ($p = 0.08$) (Figure S5 C). Additionally, we used nanoparticle-tracking analysis to measure the number and size distribution of EVs in the plasma of COVID-19 and control PFP. In agreement with the electron microscopy data, most EVs were in the 50 to 200 nm size range (Figure S5 D). When analyzed for size distribution, there was a significant increase in the number of EVs between 151–500 nM in size in COVID-19 plasma compared with control plasma ($p < 0.05$) but no differences in the 0–150 nM or 501–1000 nM size ranges (Figure S5 E). Immunoblotting demonstrated the presence of the platelet marker CD41 (integrin αIIb) in EVs isolated from both COVID-19 patients and controls (Figure S5 F). Per MISEV guidelines,[72] we performed immunoblots to examine markers of exosomes and ectosomes. The EVs stained robustly for CD63 and Tsg101, but only faintly for ARF6 (Figure S5 F), suggesting that the isolated EV pool contained more exosomes than ectosomes [72, 73]. EVs isolated from control or COVID-19 PFP were further characterized by flow cytometry (Figure S5 G). A majority of the EVs from both controls and COVID-19 patients stained positively for both annexin V binding

and CD41 (Figure S5 H). There were higher concentrations of total EVs ($p < 0.01$) (Figure S5 I), annexin V-positive EVs ($p < 0.001$) (Figure S5 J), and CD41/annexin V-double positive EVs ($p < 0.001$) (Figure S5 K) in COVID-19 PFP compared to control PFP. Taken together, these findings indicate that COVID-19 patients have elevated plasma levels of EVs, including PEVs.

Since the EVs isolated from COVID-19 plasma contain negatively charged phospholipid surfaces (demonstrated by annexin V binding), we next sought to determine whether they can accentuate thrombin generation in the absence of platelets. We first determined the contribution of endogenous EVs to thrombin generation in CTI-treated PFP triggered by TF alone (i.e., in the absence of exogenous phospholipids). Under these conditions, we observed increased thrombin generation with COVID-19 PFP compared to control PFP, reflected by increased peak thrombin, velocity index, Tmax, and ETP (Figure 6 A). To determine if procoagulant EVs were responsible for the increased thrombin generation observed with COVID-19 plasma, we depleted EVs from control and COVID-19 PFP by ultracentrifugation and when triggered by TF alone, thrombin generation was nearly absent in both groups (Figure 6 B). Further confirmation of the procoagulant effect of COVID-19 EVs was obtained when EVs isolated from equivalent volumes of control or COVID-19 patient plasma were resuspended into healthy pooled PFP and triggered with TF alone; there was a substantial increase in peak thrombin and velocity index with COVID-19 EVs compared to EVs from controls ($p < 0.05$) (Figure 6 C–E). Similar effects were observed when an equal number of control and COVID-19 EVs (normalized based on counts obtained with flow cytometry) were added to healthy pooled PFP and triggered with TF (Figure 6 F). Peak thrombin and velocity index nearly doubled with EVs from COVID-19 PFP compared to EVs from control PFP ($p < 0.05$) (Figure 6 G–H). Together, these data suggest that EVs in COVID-19 plasma are not only more numerous, but also more procoagulant, than EVs in control plasma.

EVs from COVID-19 plasma increase venous thrombosis *in vivo*

To determine the prothrombotic potential of COVID-19 EVs in a model of venous thrombosis *in vivo*, isolated EVs from equal volumes of COVID-19 PFP or control PFP were infused into 8–12-week-old C57Bl6/J mice immediately after partial ligation of the inferior vena cava. Mice infused with EVs from COVID-19 patients had larger venous thrombi 48 hours after ligation compared to mice receiving saline or EVs from controls (Figure 7 A–C). To address the possibility that histones present in isolated EVs[72] might have contributed to thrombus development in mice, we measured the levels of H3Cit in paired samples of EV-depleted PFP and isolated EVs (Figure S6). Although levels of H3Cit were higher in the EV-depleted plasma from COVID-19 patients compared to healthy controls ($p < 0.05$), H3Cit was not detectable in the washed EVs from either COVID-19 or control samples.

cfDNA does not contribute to enhanced thrombin generation in COVID-19

Patients with COVID-19 have elevated plasma levels of not only histones and nucleosomes, but also cfDNA. Since cfDNA can potentiate thrombin generation via activation of factor XII [49], we determined if cfDNA contributes to enhanced thrombin generation potential

in COVID-19. PFP from controls or COVID-19 patients was incubated with either DNase 1 or heat-inactivated DNase 1, and thrombin generation was triggered by exogenous TF and phospholipids in the absence of CTI and platelets. Under these conditions, we observed that treatment with DNase 1 did not alter thrombin generation potential in PFP from either COVID-19 patients or controls (Figure S7). These findings indicate that the enhanced thrombin generation seen in COVID-19 is not mediated by an effect of cfDNA on factor XIIa or the contact pathway of coagulation.

Discussion

Although COVID-19 is recognized as a thrombo-inflammatory illness [1–4], the mechanistic drivers of thrombin generation and thrombosis are not fully characterized. Endotheliopathy [9, 10], platelet activation [9, 11, 12], cytokine storm [13–17], NETosis [18–20], complement activation [18] and the presence of anti-phospholipid antibodies [21] have been proposed as potential mediators of the prothrombotic state in COVID-19. In this work, we demonstrate that extracellular histones, a downstream product of all of above pathways [23, 24, 26, 27], are elevated in COVID-19 plasma and cause platelet activation, platelet-dependent thrombin generation, *in vitro* thrombus formation, and procoagulant EV production. As such, extracellular histones may represent a targetable unifying mechanism driving the thrombo-inflammatory state of COVID-19 (Figure 8).

We found that plasma from COVID-19 patients promoted platelet integrin activation and PS exposure, platelet-dependent thrombin generation, and platelet thrombus formation. These prothrombotic effects of COVID-19 plasma were inhibited by HBA7, an RNA aptamer that selectively neutralizes histones. Second, we observed that COVID-19 plasma caused increased production of PEVs; this effect was also neutralized by HBA7. Further, we made the novel observation that PEV generation was stimulated by both free (histone H3 and H3Cit) and DNA-bound histones (nucleosomes), and PEV generation by H3 or H3Cit was blocked by an anti-TLR2 antibody. Platelet integrin activation and PS exposure were also inhibited by anti-TLR2 antibody, suggesting that extracellular histones in COVID-19 plasma mediate their effects on platelets via TLR2. Finally, we observed that procoagulant EVs in COVID-19 plasma enhanced thrombin generation *in vitro* and exacerbated venous thrombosis *in vivo* in a mouse model. Our findings suggest a model in which high levels of circulating extracellular histones stimulate the formation of procoagulant platelets and subsequent release of PEVs via TLR2, leading to platelet-dependent thrombin generation and thrombosis in patients with COVID-19. The effects of histones on platelets may promote thrombosis by driving the formation of both fibrin (via enhanced thrombin generation mediated by PS exposure on activated platelets and release of PEVs) and platelet thrombi (via enhanced platelet aggregation mediated by integrin αIIbβ3 activation).

In agreement with prior studies [14, 20, 22, 32–35], we observed significantly elevated levels of H3Cit and nucleosomes in plasma from COVID-19 patients. Although extracellular histones can enter the circulation from multiple sources [23, 28–31], it is likely that a major source of both free- and DNA-bound histones in COVID-19 plasma is from ETs released by neutrophils (NETs) in response to the SARS-CoV-2 spike protein or indirectly through cytokines, autoantibodies, or complement activation [18–20]. SARS-CoV-2 spike protein

can directly induce the release of NETs [65], a process that is significantly enhanced by the presence of activated platelets or PEVs [65]. These observations suggest a mechanism in which spike protein triggers NETosis, leading to a rise in extracellular histones which activate platelets through TLR2 or other receptors, resulting in procoagulant platelets and PEVs that fuel thrombin generation and further NETosis. Consistent with this mechanism, we found that plasma levels of H3Cit and nucleosomes were positively associated with mortality in our cohort of hospitalized COVID-19 patients. Furthermore, the generation of PEVs in the presence of COVID-19 plasma was completely inhibited by HBA7, and the PEV generation correlated positively with levels of H3Cit and nucleosomes in COVID-19 plasma.

Interestingly, we observed that the free histones H3 and H3Cit promoted PEV formation via TLR2, whereas nucleosomes appeared to induce PEV formation in a TLR2- and TLR4-independent manner and with a relatively higher potency than free histones. These observations suggest that DNA-bound histones may be more prothrombotic than free histones, but this possibility needs to be confirmed in future studies. We also observed elevated plasma levels of cfDNA, another product of NETosis, in COVID-19 plasma. Since cfDNA can directly activate factor XII [49, 60, 74] and has been proposed to contributed to pulmonary thrombo-inflammation in COVID-19 [75], we considered the possibility that cfDNA may promote thrombin generation in COVID-19 through the contact activation pathway of coagulation. We found, however, that thrombin generation potential in the plasma of COVID-19 patients was not altered by DNase 1, suggesting that the enhanced thrombin generation potential of COVID-19 plasma is not mediated by cfDNA.

Through a systematic approach of EV depletion and supplementation, we confirmed that the EV fraction of COVID-19 plasma is responsible for increased thrombin generation triggered by TF in the absence of platelets. These results are consistent with prior reports of EV-associated thrombin generation in plasma from COVID-19 patients [9, 70, 76] and with prior findings that PS on EVs correlates with disease severity [66, 77]. We also observed that infusion of EVs (likely produced from histone stimulation of platelets and other cells) from COVID-19 plasma enhanced the size of venous thrombi induced by partial ligation of the inferior vena cava in a mouse model, confirming prothrombotic effect of EVs in determining thrombus size *in vivo*. Similar to prior studies [9, 64–68], we detected elevated circulating levels of total EVs, annexin V-positive EVs, and CD41-positive PEVs in COVID-19 plasma. The demonstration of procoagulant PEVs in COVID-19 plasma is concordant with our findings that extracellular histones promote prothrombotic platelet activation, PEV formation and platelet-dependent thrombin generation. Our data indicate that both PS-positive platelets and PEVs can enhance thrombin generation potential, but their relative contributions to the prothrombotic state of COVID-19 remain to be determined. EVs derived from other cell types, such as neutrophils, monocytes, and endothelial cells [76], some of which contain TF [78–80], are also known to contribute to the circulating pool of EVs in COVID-19 and likely contribute to thrombosis risk as well.

Our study has a few limitations, some of which raise interesting questions for future investigation. First, the samples we studied were collected between April 2020 and January 2021, prior to the emergence of SARS-CoV-2 variants such as delta and omicron,

which may vary in their effects on hemostasis and thrombosis. However, elevation of extracellular histones has been a persistent feature of COVID-19 throughout the pandemic [37], suggesting the potential therapeutic utility of targeting extracellular histones even with the emergence of newer COVID-19 subvariants. Second, the control subjects and COVID-19 patients were not matched with respect to age, hospitalization and other clinical characteristics. The choice of control group is an inherent limitation of studies such as this one. We chose a study design in which the controls were healthy subjects to provide a reference for "normal" thrombin generation responses. Importantly, we did not observe any significant effects of age, BMI, or sex on the ability of COVID-19 plasma to promote thrombin generation, *in vitro* thrombus formation, or PEV formation (Figure S1). Moreover, most of the statistical analysis involved comparisons within the control or COVID-19 groups rather than between groups. With regards to hospitalization and other clinical characteristics, it may be interesting in future studies to compare thrombin generation in patients hospitalized with COVID-19 to those hospitalized for other infections (such as Influenza). Third, our studies of *in vitro* platelet thrombus growth were performed using healthy control platelets with stored plasma samples from COVID-19 patients or healthy subjects. Due to challenges associated with blood collection during the pandemic, we were not able to perform these experiments using fresh whole blood or cellular blood components and therefore cannot exclude potential prothrombotic effects of COVID-19 on white blood cells or erythrocytes. Lastly, although it might have been interesting to determine if the HBA7 aptamer can prevent thrombosis induced by COVID-19 EVs in the murine venous thrombosis *in vivo,* this was not possible because the prothrombotic effects of histones are upstream of EV formation. Potentially, this question and the role of TLR2 could be addressed in future studies using mouse models of COVID-19 with TLR2 knockout platelets.

Overall, our findings suggest that the pharmacological targeting of extracellular histones have therapeutic potential in COVID-19 because of their ability to influence platelet-dependent thrombosis, regardless of the upstream mechanism resulting in increased histones in the plasma.

Supplementary Material

Refer to Web version on PubMed Central for supplementary material.

Acknowledgements

This work was supported by funding from National Institutes of Health awards R01 AI162778, R01 AG049784, and T32 HL007344, Department of Veterans Affairs grants I01CX001932, American Heart Association awards 19TPA34900002 and 24POST1195019, and a pilot grant from the Roy J. Carver Charitable Trust. We acknowledge support from University of Iowa Flow Cytometry Facility, which is funded through user fees and the generous financial support of the Carver College of Medicine, Holden Comprehensive Cancer Center, and Iowa City Veteran's Administration Medical Center. We acknowledge use of the University of Iowa Central Microscopy Research Facility, a core resource supported by the University of Iowa Vice President for Research and the Carver College of Medicine. This work utilized the Transmission Electron Microscope in the University of Iowa Central Microscopy Research Facilities that was purchased with funding from National Institutes of Health award S10 RR018998-01. We acknowledge the utilization of the ViewSizer 3000 (HORIBA Scientific) at the Central Microscopy Research Facility for measuring EV sizes. The research reported in this publication was also supported by the National Center for Advancing Translational Sciences of the National Institutes of Health under Award Number UM1TR004403.

Clinical data were collected and managed using REDCap electronic data capture tools hosted at the University of Iowa Institute for Clinical and Translational Science. We acknowledge Diagnostica Stago Inc., (Parsippany NJ) for loaning a Fluoroskan Ascent instrument for thrombin generation assays. Additionally, we acknowledge Constance Shelsky for her aid in collecting healthy control samples.

References

1. Guan WJ, Zhong NS. Clinical Characteristics of Covid-19 in China. Reply. N Engl J Med. 2020;382(19):1861–2. doi: 10.1056/NEJMc2005203. [PubMed: 32220206]
2. Tang N, Li D, Wang X, Sun Z. Abnormal coagulation parameters are associated with poor prognosis in patients with novel coronavirus pneumonia. J Thromb Haemost. 2020;18(4):844–7. doi: 10.1111/jth.14768. [PubMed: 32073213]
3. Zhou F, Yu T, Du R, Fan G, Liu Y, Liu Z, et al. Clinical course and risk factors for mortality of adult inpatients with COVID-19 in Wuhan, China: a retrospective cohort study. Lancet. 2020;395(10229):1054–62. Epub 2020/03/15. doi: 10.1016/S0140-6736(20)30566-3. [PubMed: 32171076]
4. Klok FA, Kruip M, van der Meer NJM, Arbous MS, Gommers D, Kant KM, et al. Confirmation of the high cumulative incidence of thrombotic complications in critically ill ICU patients with COVID-19: An updated analysis. Thromb Res. 2020;191:148–50. doi: 10.1016/j.thromres.2020.04.041. [PubMed: 32381264]
5. Jimenez D, Garcia-Sanchez A, Rali P, Muriel A, Bikdeli B, Ruiz-Artacho P, et al. Incidence of VTE and Bleeding Among Hospitalized Patients With Coronavirus Disease 2019: A Systematic Review and Meta-analysis. Chest. 2021;159(3):1182–96. Epub 2020/11/21. doi: 10.1016/j.chest.2020.11.005. [PubMed: 33217420]
6. Wu T, Zuo Z, Yang D, Luo X, Jiang L, Xia Z, et al. Venous thromboembolic events in patients with COVID-19: a systematic review and meta-analysis. Age Ageing. 2021;50(2):284–93. Epub 2020/11/18. doi: 10.1093/ageing/afaa259. [PubMed: 33201226]
7. Mansory EM, Srigunapalan S, Lazo-Langner A. Venous Thromboembolism in Hospitalized Critical and Noncritical COVID-19 Patients: A Systematic Review and Meta-analysis. TH Open. 2021;5(3):e286–e94. Epub 2021/07/10. doi: 10.1055/s-0041-1730967. [PubMed: 34240001]
8. Kollias A, Kyriakoulis KG, Lagou S, Kontopantelis E, Stergiou GS, Syrigos K. Venous thromboembolism in COVID-19: A systematic review and meta-analysis. Vasc Med. 2021;26(4):415–25. Epub 2021/04/06. doi: 10.1177/1358863X21995566. [PubMed: 33818197]
9. Canzano P, Brambilla M, Porro B, Cosentino N, Tortorici E, Vicini S, et al. Platelet and Endothelial Activation as Potential Mechanisms Behind the Thrombotic Complications of COVID-19 Patients. JACC Basic Transl Sci. 2021;6(3):202–18. Epub 2021/03/03. doi: 10.1016/j.jacbts.2020.12.009. [PubMed: 33649738]
10. Delrue M, Siguret V, Neuwirth M, Joly B, Beranger N, Sene D, et al. von Willebrand factor/ADAMTS13 axis and venous thromboembolism in moderate-to-severe COVID-19 patients. Br J Haematol. 2021;192(6):1097–100. Epub 2020/12/29. doi: 10.1111/bjh.17216. [PubMed: 33368196]
11. Hottz ED, Azevedo-Quintanilha IG, Palhinha L, Teixeira L, Barreto EA, Pao CRR, et al. Platelet activation and platelet-monocyte aggregate formation trigger tissue factor expression in patients with severe COVID-19. Blood. 2020;136(11):1330–41. Epub 2020/07/18. doi: 10.1182/blood.2020007252. [PubMed: 32678428]
12. Manne BK, Denorme F, Middleton EA, Portier I, Rowley JW, Stubben C, et al. Platelet gene expression and function in patients with COVID-19. Blood. 2020;136(11):1317–29. Epub 2020/06/24. doi: 10.1182/blood.2020007214. [PubMed: 32573711]
13. de Vries F, Huckriede J, Wichapong K, Reutelingsperger C, Nicolaes GAF. The role of extracellular histones in COVID-19. J Intern Med. 2023;293(3):275–92. Epub 2022/11/17. doi: 10.1111/joim.13585. [PubMed: 36382685]
14. Aymonnier K, Ng J, Fredenburgh LE, Zambrano-Vera K, Munzer P, Gutch S, et al. Inflammasome activation in neutrophils of patients with severe COVID-19. Blood Adv. 2022;6(7):2001–13. Epub 2022/01/07. doi: 10.1182/bloodadvances.2021005949. [PubMed: 34991159]

15. Wolf A KF, Yoon B, Gerhart C, Endsley D, Ray AK, Yango AF, Flynn SD, Lip GYH, Gonzalez SA, Sathyamoorthy M. The mechanistic basis linking cytokine storm to thrombosis in COVID-19. Thrombosis Update. 2022;8.

16. Potere N, Garrad E, Kanthi Y, Di Nisio M, Kaplanski G, Bonaventura A, et al. NLRP3 inflammasome and interleukin-1 contributions to COVID-19-associated coagulopathy and immunothrombosis. Cardiovasc Res. 2023. Epub 2023/05/30. doi: 10.1093/cvr/cvad084.

17. Smilowitz NR, Kunichoff D, Garshick M, Shah B, Pillinger M, Hochman JS, Berger JS. C-reactive protein and clinical outcomes in patients with COVID-19. Eur Heart J. 2021;42(23):2270–9. Epub 2021/01/16. doi: 10.1093/eurheartj/ehaa1103. [PubMed: 33448289]

18. Skendros P, Mitsios A, Chrysanthopoulou A, Mastellos DC, Metallidis S, Rafailidis P, et al. Complement and tissue factor-enriched neutrophil extracellular traps are key drivers in COVID-19 immunothrombosis. J Clin Invest. 2020;130(11):6151–7. Epub 2020/08/08. doi: 10.1172/JCI141374. [PubMed: 32759504]

19. Middleton EA, He XY, Denorme F, Campbell RA, Ng D, Salvatore SP, et al. Neutrophil extracellular traps contribute to immunothrombosis in COVID-19 acute respiratory distress syndrome. Blood. 2020;136(10):1169–79. doi: 10.1182/blood.2020007008. [PubMed: 32597954]

20. Zuo Y, Yalavarthi S, Shi H, Gockman K, Zuo M, Madison JA, et al. Neutrophil extracellular traps in COVID-19. JCI Insight. 2020;5(11). Epub 2020/04/25. doi: 10.1172/jci.insight.138999.

21. Zuo Y, Estes SK, Ali RA, Gandhi AA, Yalavarthi S, Shi H, et al. Prothrombotic autoantibodies in serum from patients hospitalized with COVID-19. Sci Transl Med. 2020;12(570). Epub 2020/11/04. doi: 10.1126/scitranslmed.abd3876.

22. Zuo Y, Zuo M, Yalavarthi S, Gockman K, Madison JA, Shi H, et al. Neutrophil extracellular traps and thrombosis in COVID-19. J Thromb Thrombolysis. 2021;51(2):446–53. Epub 2020/11/06. doi: 10.1007/s11239-020-02324-z. [PubMed: 33151461]

23. Ramos-Martinez E, Hernandez-Gonzalez L, Ramos-Martinez I, Perez-Campos Mayoral L, Lopez-Cortes GI, Perez-Campos E, et al. Multiple Origins of Extracellular DNA Traps. Front Immunol. 2021;12:621311. Epub 2021/03/16. doi: 10.3389/fimmu.2021.621311. [PubMed: 33717121]

24. Keshari RS, Jyoti A, Dubey M, Kothari N, Kohli M, Bogra J, et al. Cytokines induced neutrophil extracellular traps formation: implication for the inflammatory disease condition. PLoS One. 2012;7(10):e48111. Epub 20121026. doi: 10.1371/journal.pone.0048111. [PubMed: 23110185]

25. Chen SY, Wang CT, Chen CY, Kuo PY, Wang CR, Shiau AL, et al. Galectin-3 Mediates NETosis and Acts as an Autoantigen in Systemic Lupus Erythematosus-Associated Diffuse Alveolar Haemorrhage. Int J Mol Sci. 2023;24(11). Epub 2023/06/10. doi: 10.3390/ijms24119493.

26. Maugeri N, Campana L, Gavina M, Covino C, De Metrio M, Panciroli C, et al. Activated platelets present high mobility group box 1 to neutrophils, inducing autophagy and promoting the extrusion of neutrophil extracellular traps. J Thromb Haemost. 2014;12(12):2074–88. Epub 2014/08/29. doi: 10.1111/jth.12710. [PubMed: 25163512]

27. Gupta AK, Joshi MB, Philippova M, Erne P, Hasler P, Hahn S, Resink TJ. Activated endothelial cells induce neutrophil extracellular traps and are susceptible to NETosis-mediated cell death. FEBS Lett. 2010;584(14):3193–7. Epub 2010/06/15. doi: 10.1016/j.febslet.2010.06.006. [PubMed: 20541553]

28. Fuchs TA, Abed U, Goosmann C, Hurwitz R, Schulze I, Wahn V, et al. Novel cell death program leads to neutrophil extracellular traps. J Cell Biol. 2007;176(2):231–41. doi: 10.1083/jcb.200606027. [PubMed: 17210947]

29. Radic M, Marion T, Monestier M. Nucleosomes are exposed at the cell surface in apoptosis. J Immunol. 2004;172(11):6692–700. Epub 2004/05/22. doi: 10.4049/jimmunol.172.11.6692. [PubMed: 15153485]

30. Granger V, Faille D, Marani V, Noel B, Gallais Y, Szely N, et al. Human blood monocytes are able to form extracellular traps. J Leukoc Biol. 2017;102(3):775–81. Epub 2017/05/04. doi: 10.1189/jlb.3MA0916-411R. [PubMed: 28465447]

31. Muniz VS, Silva JC, Braga YAV, Melo RCN, Ueki S, Takeda M, et al. Eosinophils release extracellular DNA traps in response to Aspergillus fumigatus. J Allergy Clin Immunol. 2018;141(2):571–85 e7. Epub 2017/09/26. doi: 10.1016/j.jaci.2017.07.048. [PubMed: 28943470]

32. Cavalier E, Guiot J, Lechner K, Dutsch A, Eccleston M, Herzog M, et al. Circulating Nucleosomes as Potential Markers to Monitor COVID-19 Disease Progression. Front Mol Biosci. 2021;8:600881. Epub 2021/04/06. doi: 10.3389/fmolb.2021.600881. [PubMed: 33816549]
33. Godement M, Zhu J, Cerf C, Vieillard-Baron A, Maillon A, Zuber B, et al. Neutrophil Extracellular Traps in SARS-CoV2 Related Pneumonia in ICU Patients: The NETCOV2 Study. Front Med (Lausanne). 2021;8:615984. Epub 20210223. doi: 10.3389/fmed.2021.615984. [PubMed: 33708778]
34. Huckriede J, de Vries F, Hultstrom M, Wichapong K, Reutelingsperger C, Lipcsey M, et al. Histone H3 Cleavage in Severe COVID-19 ICU Patients. Front Cell Infect Microbiol. 2021;11:694186. Epub 20210910. doi: 10.3389/fcimb.2021.694186. [PubMed: 34568088]
35. Ng H, Havervall S, Rosell A, Aguilera K, Parv K, von Meijenfeldt FA, et al. Circulating Markers of Neutrophil Extracellular Traps Are of Prognostic Value in Patients With COVID-19. Arterioscler Thromb Vasc Biol. 2021;41(2):988–94. Epub 2020/12/04. doi: 10.1161/ATVBAHA.120.315267. [PubMed: 33267662]
36. Veras FP, Pontelli MC, Silva CM, Toller-Kawahisa JE, de Lima M, Nascimento DC, et al. SARS-CoV-2-triggered neutrophil extracellular traps mediate COVID-19 pathology. J Exp Med. 2020;217(12). doi: 10.1084/jem.20201129.
37. Ligi D, Giglio RV, Henry BM, Lippi G, Ciaccio M, Plebani M, Mannello F. What is the impact of circulating histones in COVID-19: a systematic review. Clin Chem Lab Med. 2022. Epub 2022/07/20. doi: 10.1515/cclm-2022-0574.
38. Xu J, Zhang X, Pelayo R, Monestier M, Ammollo CT, Semeraro F, et al. Extracellular histones are major mediators of death in sepsis. Nat Med. 2009;15(11):1318–21. Epub 2009/10/27. doi: 10.1038/nm.2053. [PubMed: 19855397]
39. Xu J, Zhang X, Monestier M, Esmon NL, Esmon CT. Extracellular histones are mediators of death through TLR2 and TLR4 in mouse fatal liver injury. J Immunol. 2011;187(5):2626–31. Epub 2011/07/26. doi: 10.4049/jimmunol.1003930. [PubMed: 21784973]
40. Ammollo CT, Semeraro F, Xu J, Esmon NL, Esmon CT. Extracellular histones increase plasma thrombin generation by impairing thrombomodulin-dependent protein C activation. J Thromb Haemost. 2011;9(9):1795–803. doi: 10.1111/j.1538-7836.2011.04422.x. [PubMed: 21711444]
41. Michels A, Albanez S, Mewburn J, Nesbitt K, Gould TJ, Liaw PC, et al. Histones link inflammation and thrombosis through the induction of Weibel-Palade body exocytosis. J Thromb Haemost. 2016;14(11):2274–86. Epub 2016/09/03. doi: 10.1111/jth.13493. [PubMed: 27589692]
42. Kim JE, Yoo HJ, Gu JY, Kim HK. Histones Induce the Procoagulant Phenotype of Endothelial Cells through Tissue Factor Up-Regulation and Thrombomodulin Down-Regulation. PLoS One. 2016;11(6):e0156763. Epub 2016/06/04. doi: 10.1371/journal.pone.0156763. [PubMed: 27258428]
43. Zhang Y, Wu C, Li L, Pandeya A, Zhang G, Cui J, et al. Extracellular Histones Trigger Disseminated Intravascular Coagulation by Lytic Cell Death. Int J Mol Sci. 2022;23(12). Epub 2022/06/25. doi: 10.3390/ijms23126800.
44. Shah M, He Z, Rauf A, Beikoghli Kalkhoran S, Heiestad CM, Stenslokken KO, et al. Extracellular histones are a target in myocardial ischaemia-reperfusion injury. Cardiovasc Res. 2022;118(4):1115–25. Epub 2021/04/21. doi: 10.1093/cvr/cvab139. [PubMed: 33878183]
45. De Meyer SF, Suidan GL, Fuchs TA, Monestier M, Wagner DD. Extracellular chromatin is an important mediator of ischemic stroke in mice. Arterioscler Thromb Vasc Biol. 2012;32(8):1884–91. doi: 10.1161/ATVBAHA.112.250993. [PubMed: 22628431]
46. Valles J, Lago A, Santos MT, Latorre AM, Tembl JI, Salom JB, et al. Neutrophil extracellular traps are increased in patients with acute ischemic stroke: prognostic significance. Thromb Haemost. 2017;117(10):1919–29. Epub 2017/08/25. doi: 10.1160/TH17-02-0130. [PubMed: 28837206]
47. Demyanets S, Stojkovic S, Mauracher LM, Kopp CW, Wojta J, Thaler J, et al. Surrogate Markers of Neutrophil Extracellular Trap Formation are Associated with Ischemic Outcomes and Platelet Activation after Peripheral Angioplasty and Stenting. J Clin Med. 2020;9(2). Epub 20200122. doi: 10.3390/jcm9020304.

48. Brill A, Fuchs TA, Savchenko AS, Thomas GM, Martinod K, De Meyer SF, et al. Neutrophil extracellular traps promote deep vein thrombosis in mice. J Thromb Haemost. 2012;10(1):136–44. doi: 10.1111/j.1538-7836.2011.04544.x. [PubMed: 22044575]

49. Gould TJ, Vu TT, Swystun LL, Dwivedi DJ, Mai SH, Weitz JI, Liaw PC. Neutrophil extracellular traps promote thrombin generation through platelet-dependent and platelet-independent mechanisms. Arterioscler Thromb Vasc Biol. 2014;34(9):1977–84. doi: 10.1161/ATVBAHA.114.304114. [PubMed: 25012129]

50. Semeraro F, Ammollo CT, Morrissey JH, Dale GL, Friese P, Esmon NL, Esmon CT. Extracellular histones promote thrombin generation through platelet-dependent mechanisms: involvement of platelet TLR2 and TLR4. Blood. 2011;118(7):1952–61. doi: 10.1182/blood-2011-03-343061. [PubMed: 21673343]

51. Nougier C, Benoit R, Simon M, Desmurs-Clavel H, Marcotte G, Argaud L, et al. Hypofibrinolytic state and high thrombin generation may play a major role in SARS-COV2 associated thrombosis. J Thromb Haemost. 2020;18(9):2215–9. Epub 2020/07/16. doi: 10.1111/jth.15016. [PubMed: 32668058]

52. White D, MacDonald S, Edwards T, Bridgeman C, Hayman M, Sharp M, et al. Evaluation of COVID-19 coagulopathy; laboratory characterization using thrombin generation and nonconventional haemostasis assays. Int J Lab Hematol. 2021;43(1):123–30. Epub 2020/09/07. doi: 10.1111/ijlh.13329. [PubMed: 32892505]

53. Bouck EG, Denorme F, Holle LA, Middelton EA, Blair AM, de Laat B, et al. COVID-19 and Sepsis Are Associated With Different Abnormalities in Plasma Procoagulant and Fibrinolytic Activity. Arterioscler Thromb Vasc Biol. 2021;41(1):401–14. Epub 2020/11/17. doi: 10.1161/ATVBAHA.120.315338. [PubMed: 33196292]

54. Campello E, Bulato C, Spiezia L, Boscolo A, Poletto F, Cola M, et al. Thrombin generation in patients with COVID-19 with and without thromboprophylaxis. Clin Chem Lab Med. 2021;59(7):1323–30. Epub 2021/02/06. doi: 10.1515/cclm-2021-0108. [PubMed: 33544518]

55. Perepu US, Chambers I, Wahab A, Ten Eyck P, Wu C, Dayal S, et al. Standard prophylactic versus intermediate dose enoxaparin in adults with severe COVID-19: A multi-center, open-label, randomized controlled trial. J Thromb Haemost. 2021;19(9):2225–34. Epub 2021/07/09. doi: 10.1111/jth.15450. [PubMed: 34236768]

56. Szatanek R, Baran J, Siedlar M, Baj-Krzyworzeka M. Isolation of extracellular vesicles: Determining the correct approach (Review). Int J Mol Med. 2015;36(1):11–7. Epub 2015/04/23. doi: 10.3892/ijmm.2015.2194. [PubMed: 25902369]

57. Sonkar VK, Kumar R, Jensen M, Wagner BA, Sharathkumar AA, Miller FJ, Jr., et al. Nox2 NADPH oxidase is dispensable for platelet activation or arterial thrombosis in mice. Blood Adv. 2019;3(8):1272–84. doi: 10.1182/bloodadvances.2018025569. [PubMed: 30995985]

58. Urak KT, Blanco GN, Shubham S, Lin LH, Dassie JP, Thiel WH, et al. RNA inhibitors of nuclear proteins responsible for multiple organ dysfunction syndrome. Nat Commun. 2019;10(1):116. doi: 10.1038/s41467-018-08030-y. [PubMed: 30631065]

59. Hemker HC, Giesen P, Al Dieri R, Regnault V, de Smedt E, Wagenvoord R, et al. Calibrated automated thrombin generation measurement in clotting plasma. Pathophysiol Haemost Thromb. 2003;33(1):4–15. doi: 10.1159/000071636. [PubMed: 12853707]

60. Kumar R, Sonkar VK, Swamy J, Ahmed A, Sharathkumar AA, Pierce GL, Dayal S. DNase 1 Protects From Increased Thrombin Generation and Venous Thrombosis During Aging: Cross-Sectional Study in Mice and Humans. J Am Heart Assoc. 2022;11(2):e021188. Epub 20220113. doi: 10.1161/JAHA.121.021188. [PubMed: 35023342]

61. Rasch D, Kubinger KD, and Moder K. The two-sample t test: pre-testing its assumptions does not pay off. Stat Papers. 2011;52:219–31. doi: 10.1007/s00362-009-0224-x.

62. Tripisciano C, Weiss R, Eichhorn T, Spittler A, Heuser T, Fischer MB, Weber V. Different Potential of Extracellular Vesicles to Support Thrombin Generation: Contributions of Phosphatidylserine, Tissue Factor, and Cellular Origin. Sci Rep. 2017;7(1):6522. Epub 2017/07/28. doi: 10.1038/s41598-017-03262-2. [PubMed: 28747771]

63. Aleman MM, Gardiner C, Harrison P, Wolberg AS. Differential contributions of monocyte- and platelet-derived microparticles towards thrombin generation and fibrin formation

and stability. J Thromb Haemost. 2011;9(11):2251–61. Epub 2011/09/03. doi: 10.1111/j.1538-7836.2011.04488.x. [PubMed: 21883880]

64. Traby L, Kollars M, Kussmann M, Karer M, Sinkovec H, Lobmeyr E, et al. Extracellular Vesicles and Citrullinated Histone H3 in Coronavirus Disease 2019 Patients. Thromb Haemost. 2022;122(1):113–22. Epub 2021/06/03. doi: 10.1055/a-1522-4131. [PubMed: 34077977]
65. Sung PS, Yang SP, Peng YC, Sun CP, Tao MH, Hsieh SL. CLEC5A and TLR2 are critical in SARS-CoV-2-induced NET formation and lung inflammation. J Biomed Sci. 2022;29(1):52. Epub 2022/07/13. doi: 10.1186/s12929-022-00832-z. [PubMed: 35820906]
66. Garnier Y, Claude L, Hermand P, Sachou E, Claes A, Desplan K, et al. Plasma microparticles of intubated COVID-19 patients cause endothelial cell death, neutrophil adhesion and netosis, in a phosphatidylserine-dependent manner. Br J Haematol. 2022;196(5):1159–69. Epub 2021/12/29. doi: 10.1111/bjh.18019. [PubMed: 34962643]
67. Guervilly C, Bonifay A, Burtey S, Sabatier F, Cauchois R, Abdili E, et al. Dissemination of extreme levels of extracellular vesicles: tissue factor activity in patients with severe COVID-19. Blood Adv. 2021;5(3):628–34. Epub 2021/02/10. doi: 10.1182/bloodadvances.2020003308. [PubMed: 33560376]
68. Balbi C, Burrello J, Bolis S, Lazzarini E, Biemmi V, Pianezzi E, et al. Circulating extracellular vesicles are endowed with enhanced procoagulant activity in SARS-CoV-2 infection. EBioMedicine. 2021;67:103369. Epub 2021/05/11. doi: 10.1016/j.ebiom.2021.103369. [PubMed: 33971404]
69. Brambilla M, Canzano P, Becchetti A, Tremoli E, Camera M. Letter by Brambilla et al. Regarding Article, "Patients With COVID-19 Have Elevated Levels of Circulating Extracellular Vesicle Tissue Factor Activity That Is Associated With Severity and Mortality-Brief Report". Arterioscler Thromb Vasc Biol. 2021;41(6):e379–e80. Epub 2021/05/27. doi: 10.1161/ATVBAHA.121.316188. [PubMed: 34038167]
70. Rosell A, Havervall S, von Meijenfeldt F, Hisada Y, Aguilera K, Grover SP, et al. Patients With COVID-19 Have Elevated Levels of Circulating Extracellular Vesicle Tissue Factor Activity That Is Associated With Severity and Mortality-Brief Report. Arterioscler Thromb Vasc Biol. 2021;41(2):878–82. Epub 2020/12/04. doi: 10.1161/ATVBAHA.120.315547. [PubMed: 33267656]
71. Vulliamy P, Gillespie S, Armstrong PC, Allan HE, Warner TD, Brohi K. Histone H4 induces platelet ballooning and microparticle release during trauma hemorrhage. Proc Natl Acad Sci U S A. 2019;116(35):17444–9. Epub 2019/08/14. doi: 10.1073/pnas.1904978116. [PubMed: 31405966]
72. Thery C, Witwer KW, Aikawa E, Alcaraz MJ, Anderson JD, Andriantsitohaina R, et al. Minimal information for studies of extracellular vesicles 2018 (MISEV2018): a position statement of the International Society for Extracellular Vesicles and update of the MISEV2014 guidelines. J Extracell Vesicles. 2018;7(1):1535750. Epub 20181123. doi: 10.1080/20013078.2018.1535750. [PubMed: 30637094]
73. Eustes AS, Dayal S. The Role of Platelet-Derived Extracellular Vesicles in Immune-Mediated Thrombosis. Int J Mol Sci. 2022;23(14). Epub 20220716. doi: 10.3390/ijms23147837.
74. Kumar R, Katare PB, Lentz SR, Modi AJ, Sharathkumar AA, Dayal S. Thrombotic potential during pediatric acute lymphoblastic leukemia induction: Role of cell-free DNA. Res Pract Thromb Haemost. 2021;5(5):e12557. Epub 2021/08/03. doi: 10.1002/rth2.12557. [PubMed: 34337307]
75. Englert H, Rangaswamy C, Deppermann C, Sperhake JP, Krisp C, Schreier D, et al. Defective NET clearance contributes to sustained FXII activation in COVID-19-associated pulmonary thrombo-inflammation. EBioMedicine. 2021;67:103382. Epub 2021/05/18. doi: 10.1016/j.ebiom.2021.103382. [PubMed: 34000623]
76. Mackman N, Grover SP, Antoniak S. Tissue factor expression, extracellular vesicles, and thrombosis after infection with the respiratory viruses influenza A virus and coronavirus. J Thromb Haemost. 2021;19(11):2652–8. Epub 2021/08/22. doi: 10.1111/jth.15509. [PubMed: 34418279]
77. Assimakopoulos SF, Emmanuil A, Tsimeka A, Chalkidi T, Marangos M, Gogos C. Evidence for increased circulating procoagulant phospholipids in patients with COVID-19 pneumonia and

their prognostic role. Clin Chem Lab Med. 2020;59(2):e53–e5. Epub 2020/10/29. doi: 10.1515/cclm-2020-1260. [PubMed: 33112778]

78. Eichhorn T, Weiss R, Huber S, Ebeyer-Masotta M, Mostageer M, Emprechtinger R, et al. Expression of Tissue Factor and Platelet/Leukocyte Markers on Extracellular Vesicles Reflect Platelet-Leukocyte Interaction in Severe COVID-19. Int J Mol Sci. 2023;24(23). Epub 20231128. doi: 10.3390/ijms242316886.
79. Sachetto ATA, Archibald SJ, Hisada Y, Rosell A, Havervall S, van Es N, et al. Tissue factor activity of small and large extracellular vesicles in different diseases. Res Pract Thromb Haemost. 2023;7(3):100124. Epub 20230315. doi: 10.1016/j.rpth.2023.100124. [PubMed: 37012986]
80. Girard TJ, Antunes L, Zhang N, Amrute JM, Subramanian R, Eldem I, et al. Peripheral blood mononuclear cell tissue factor (F3 gene) transcript levels and circulating extracellular vesicles are elevated in severe coronavirus 2019 (COVID-19) disease. J Thromb Haemost. 2023;21(3):629–38. Epub 20221222. doi: 10.1016/j.jtha.2022.11.033. [PubMed: 36696180]

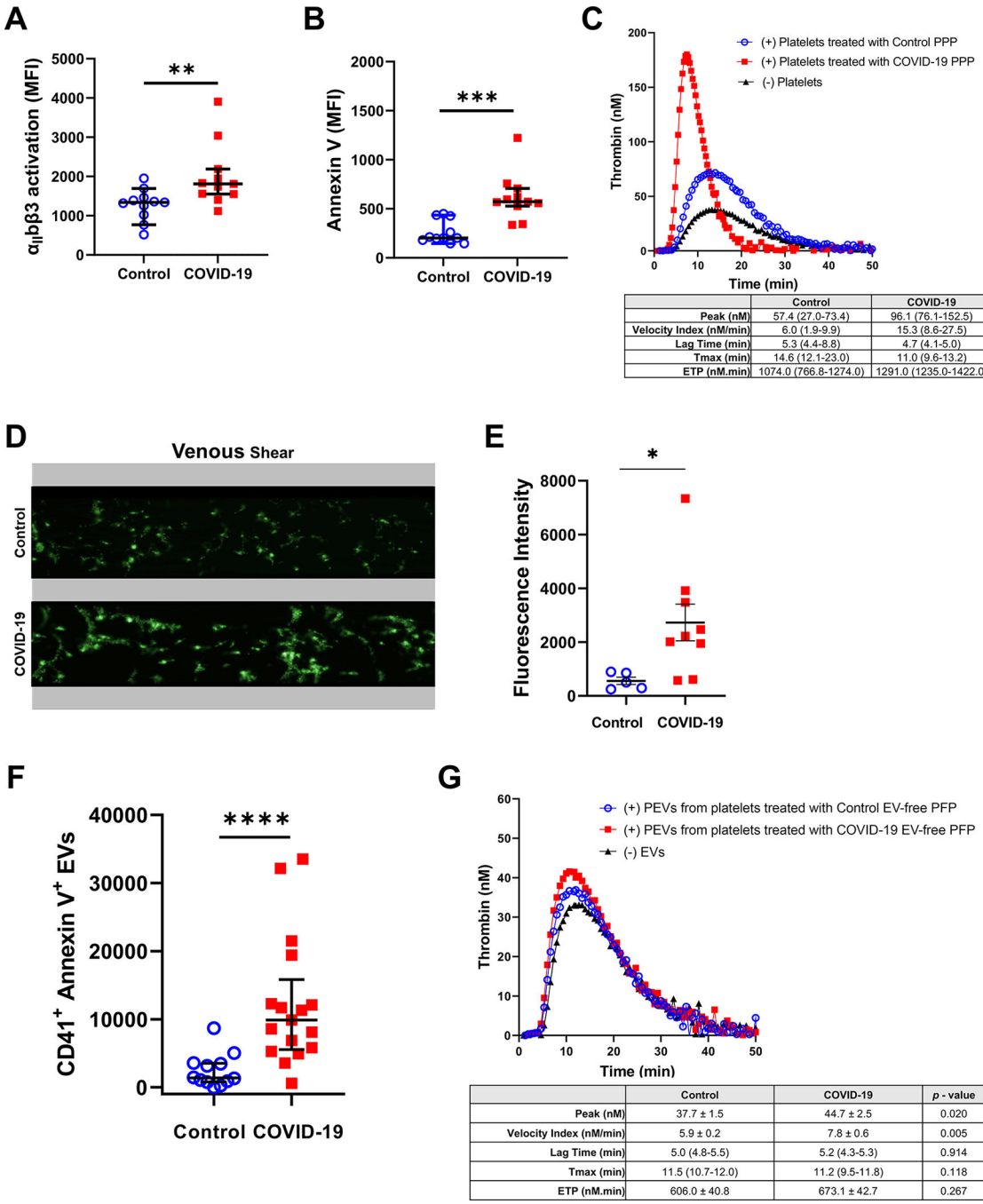

	Control	COVID-19	*p* - value
Peak (nM)	57.4 (27.0-73.4)	96.1 (76.1-152.5)	0.001
Velocity Index (nM/min)	6.0 (1.9-9.9)	15.3 (8.6-27.5)	0.002
Lag Time (min)	5.3 (4.4-8.8)	4.7 (4.1-5.0)	0.038
Tmax (min)	14.6 (12.1-23.0)	11.0 (9.6-13.2)	0.015
ETP (nM.min)	1074.0 (766.8-1274.0)	1291.0 (1235.0-1422.0)	0.006

	Control	COVID-19	*p* - value
Peak (nM)	37.7 ± 1.5	44.7 ± 2.5	0.020
Velocity Index (nM/min)	5.9 ± 0.2	7.8 ± 0.6	0.005
Lag Time (min)	5.0 (4.8-5.5)	5.2 (4.3-5.3)	0.914
Tmax (min)	11.5 (10.7-12.0)	11.2 (9.5-11.8)	0.118
ETP (nM.min)	606.0 ± 40.8	673.1 ± 42.7	0.267

Figure 1. Plasma from COVID-19 patients promotes platelet-dependent thrombin generation, thrombus formation, and PEV production.

(A & B) Washed platelets from a healthy control subject were stimulated with PPP from either control subjects (blue) (N = 11) or COVID-19 patients (red) (N = 11) for 15 minutes. After stimulation, samples were centrifuged, and platelet pellets were resuspended in Tyrode buffer, incubated with (A) PE-conjugated PAC1 or (B) annexin V-APC, samples were fixed, diluted and analyzed by flow cytometry. Data are presented as median and IQR and compared using the Mann Whitney test. **(C)** Washed platelets were isolated

from a healthy control subject and stimulated with PPP from healthy control subjects (N = 9) or COVID-19 patients (N = 25) for 15 minutes. After stimulation, platelets were centrifuged and resuspended in pooled healthy PFP containing CTI, and thrombin generation was triggered with 1 pM tissue factor (TF). Representative thrombin generation curves and quantitative data (see associated table) are presented. Black triangles represent no added platelets; blue circles represent platelets incubated with control PPP; red squares represent platelets incubated with COVID-19 plasma. Data are presented as mean and SEM for normally distributed data and median and IQR for non-normally distributed data. Comparisons were made using the unpaired t-test or the Mann Whitney test. **(D & E)** Recalcified PPP from either control subjects (N = 5) (blue) or COVID-19 patients (N = 9) (red) were incubated with calcein green-labeled platelets from control subjects and perfused over a collagen coated surface under venous shear stress (500 s^{-1}) for 10 minutes. **D** Representative images after 10 minutes. **(E)** Fluorescence intensity at the 10-minute time point was measured to account for both the area covered and changes in signal intensity due to thrombus growth in the Z direction. Data are presented as mean and SEM and comparisons were performed using an unpaired student's t-test. **(F)** Washed platelets were isolated from a healthy subject and stimulated with EV-free PFP from healthy control subjects (N = 12) or COVID-19 patients (N = 17) for 60 minutes. After stimulation, platelets were removed by centrifugation and then EVs were isolated by ultracentrifugation. EVs were stained for CD41 and annexin V binding and quantitated by flow cytometry. Data are presented as median and IQR; analysis was performed using Mann-Whitney test. **(G)** PEVs produced in the same manner as F, were isolated and added to EV-free control PFP. Thrombin generation was triggered with 1 pM TF, and representative curves are shown for PEVs from platelets stimulated with control EV-free plasma (blue open circles) (N = 24) or COVID-19 EV-free plasma (red squares) (N = 26) and the black triangles represent the baseline EV-free control PFP. Quantification is presented in associated table as mean and SEM for normally distributed data and median and IQR for non-normally distributed data. Comparisons were made using the unpaired t-test or the Mann Whitney test. * $p < 0.05$, ** $p < 0.01$, *** $p < 0.001$, **** $p < 0.0001$.

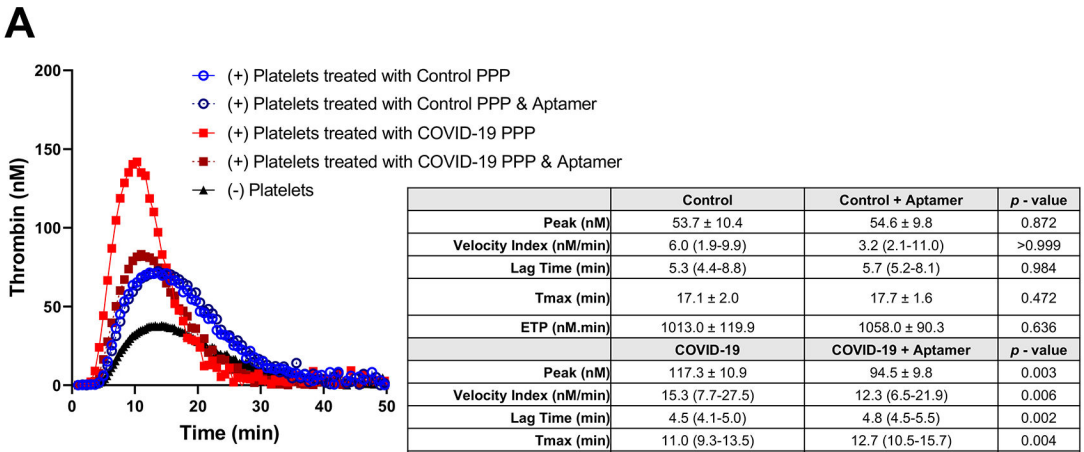

	Control	Control + Aptamer	*p* - value
Peak (nM)	53.7 ± 10.4	54.6 ± 9.8	0.872
Velocity Index (nM/min)	6.0 (1.9-9.9)	3.2 (2.1-11.0)	>0.999
Lag Time (min)	5.3 (4.4-8.8)	5.7 (5.2-8.1)	0.984
Tmax (min)	17.1 ± 2.0	17.7 ± 1.6	0.472
ETP (nM.min)	1013.0 ± 119.9	1058.0 ± 90.3	0.636
	COVID-19	**COVID-19 + Aptamer**	***p* - value**
Peak (nM)	117.3 ± 10.9	94.5 ± 9.8	0.003
Velocity Index (nM/min)	15.3 (7.7-27.5)	12.3 (6.5-21.9)	0.006
Lag Time (min)	4.5 (4.1-5.0)	4.8 (4.5-5.5)	0.002
Tmax (min)	11.0 (9.3-13.5)	12.7 (10.5-15.7)	0.004
ETP (nM.min)	1294.0 (1235.0-1434.0)	1229.0 (1168.0-1297.0)	0.074

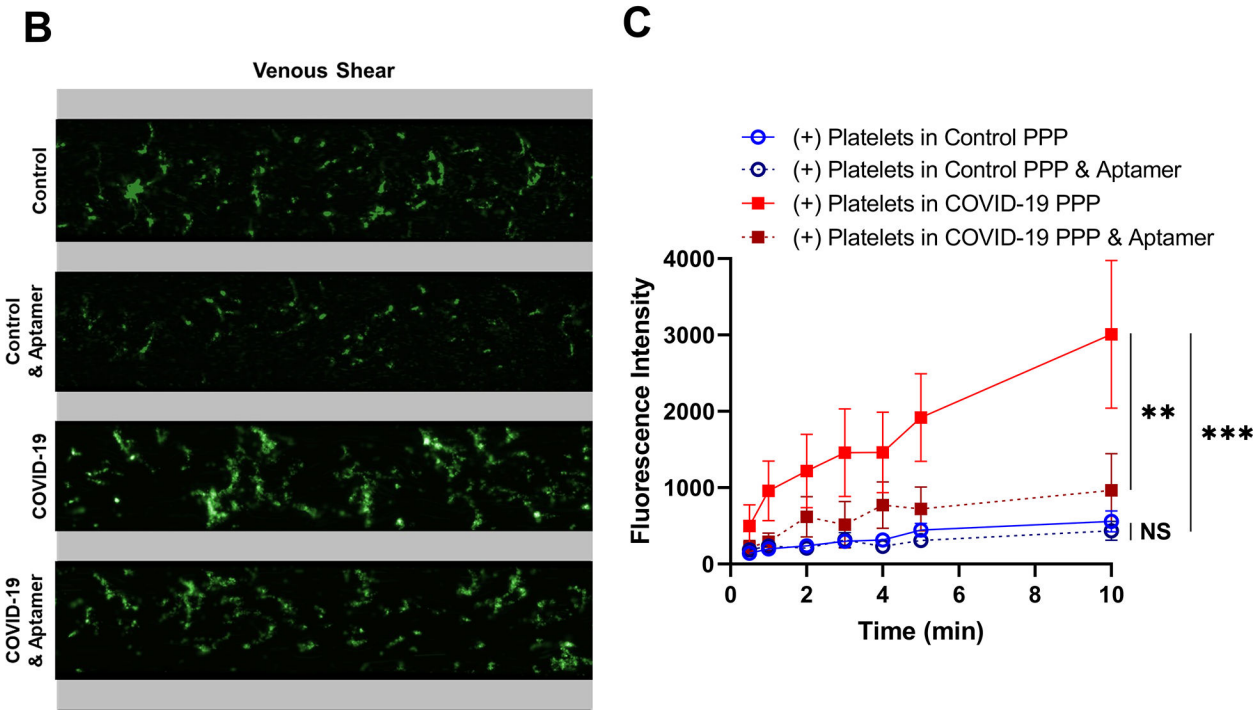

Figure 2. Extracellular histones in COVID-19 plasma promote platelet-dependent thrombin generation and thrombus formation.

(A) Washed platelets were isolated from a healthy control subject and stimulated with PPP from either control subjects (blue) (N = 9) or COVID-19 patients (red) (N = 23) for 15 minutes. PPP was incubated with the histone aptamer HBA7 (dotted lines) or vehicle (solid lines) for 5 min prior to platelet stimulation. After stimulation, samples were centrifuged and platelet pellets were resuspended in pooled healthy PFP containing CTI, and thrombin generation was triggered with 1 pM tissue factor. Representative thrombin generation curves and quantitative data (see associated table) are presented. Black arrows represent pooled healthy PFP containing CTI without added platelets. Data are presented as mean and SEM for normally distributed data and median and IQR for non-normally

distributed data. Comparisons were made using the unpaired t-test or the Mann Whitney test. **(B-C)** Recalcified PPP from either control subjects (N = 5) (blue) or COVID-19 patients (N = 6) (red) were incubated with the histone aptamer HBA7 (dotted lines) or vehicle (solid lines) for 5 min prior to the addition of washed calcein green-labeled platelets from control subjects and perfused over a collagen coated surface under shear stress (500 s^{-1}) for 10 minutes. **(B)** Representative images after 10 minutes. **(C)** Fluorescent intensity was measured to account for both the area covered and changes in signal intensity due to thrombus growth in the Z direction. Data are presented as mean and SEM and comparisons were performed using mixed effects ANOVA. ** $p < 0.01$, *** $p < 0.001$.

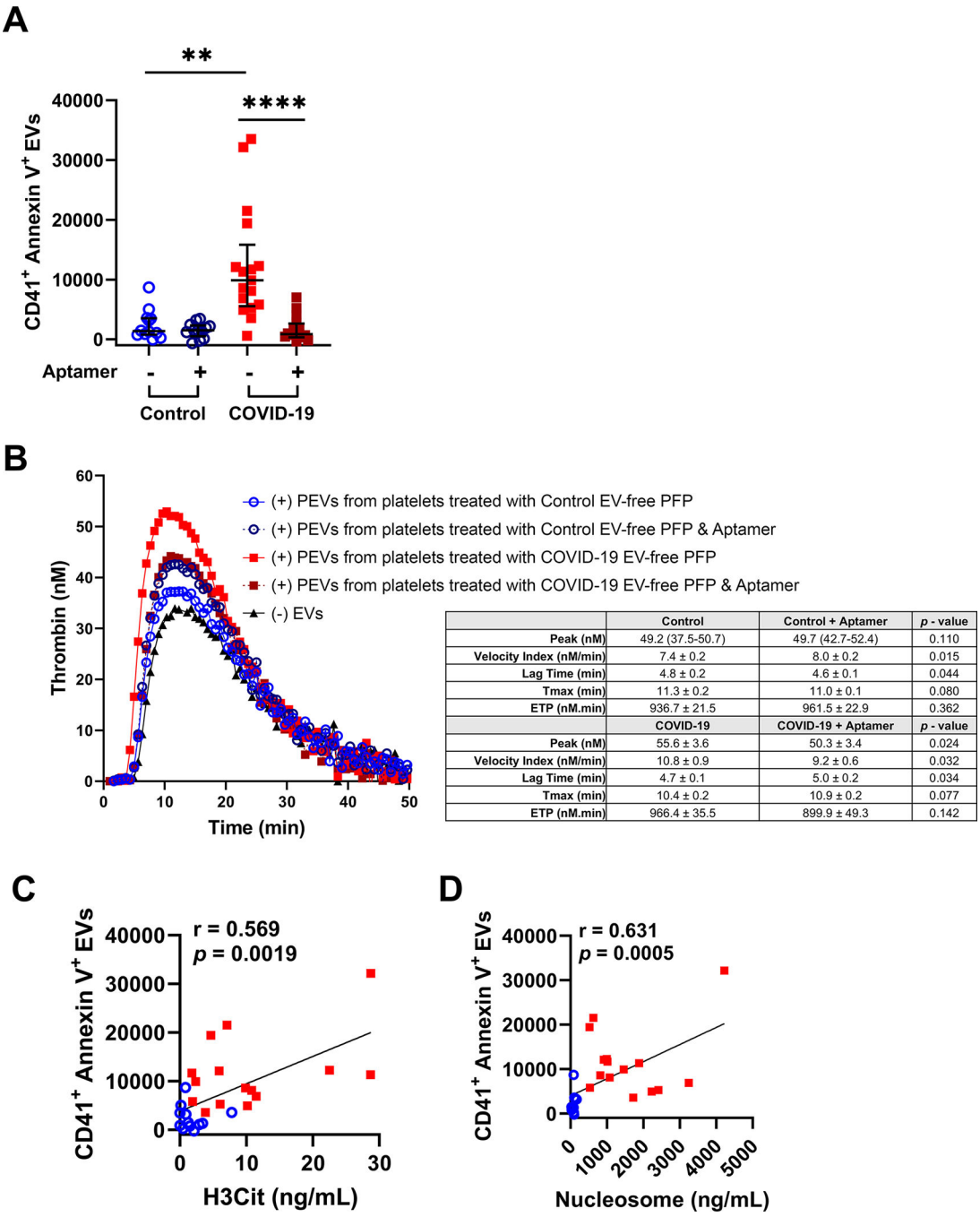

	Control	Control + Aptamer	*p* - value
Peak (nM)	49.2 (37.5-50.7)	49.7 (42.7-52.4)	0.110
Velocity Index (nM/min)	7.4 ± 0.2	8.0 ± 0.2	0.015
Lag Time (min)	4.8 ± 0.2	4.6 ± 0.1	0.044
Tmax (min)	11.3 ± 0.2	11.0 ± 0.1	0.080
ETP (nM.min)	936.7 ± 21.5	961.5 ± 22.9	0.362
	COVID-19	**COVID-19 + Aptamer**	***p* - value**
Peak (nM)	55.6 ± 3.6	50.3 ± 3.4	0.024
Velocity Index (nM/min)	10.8 ± 0.9	9.2 ± 0.6	0.032
Lag Time (min)	4.7 ± 0.1	5.0 ± 0.2	0.034
Tmax (min)	10.4 ± 0.2	10.9 ± 0.2	0.077
ETP (nM.min)	966.4 ± 35.5	899.9 ± 49.3	0.142

Figure 3: Extracellular histones in COVID-19 plasma promote PEV production.

(A) Washed platelets were isolated from a healthy subject and stimulated with EV-free plasma from control subjects (N = 13) or COVID-19 patients (N = 16) for 60 minutes. The EV-free plasma was incubated with the histone aptamer HBA7 or vehicle for 5 min prior to platelet stimulation. After stimulation, platelets were removed by centrifugation and then EVs were isolated by ultracentrifugation. EVs were stained for CD41 and annexin V binding and quantitated by flow cytometry. Data are presented as median and IQR; analysis was performed using Kruskal Wallis test with Dunns multiple comparison. **(B)** PEVs produced

in the same manner as A, were isolated and added to EV-free control PFP. HBA7 was added during the production of the PEVs and thrombin generation was triggered with 1 pM tissue factor (TF): representative curves and quantification for PEVs from platelets stimulated with control EV-free plasma (blue circles with a solid line) or control EV-free plasma containing HBA7 (blue circles with a dotted line), PEVs from platelets stimulated with COVID-19 EV-free plasma (red squares with a solid line) or COVID-19 EV-free plasma containing HBA7 (red squares with a dotted line) (N = 10 for all four conditions). The black triangles are the baseline control EV-free PFP. Data are presented as mean and SEM for normally distributed data and median and IQR for non-normally distributed data. Comparisons were made using the unpaired t-test or the Mann Whitney test. (**C-D**) Spearman correlation was performed for the number of PEVs produced (when washed platelets from healthy control subjects were incubated with EV-free PFP from control subjects or COVID-19 patients) with the plasma levels of (**C**) citrullinated histone (H3Cit) or (**D**) nucleosomes (N = 11 control and N = 15 COVID-19). ** $p < 0.01$, **** $p \leq 0.0001$.

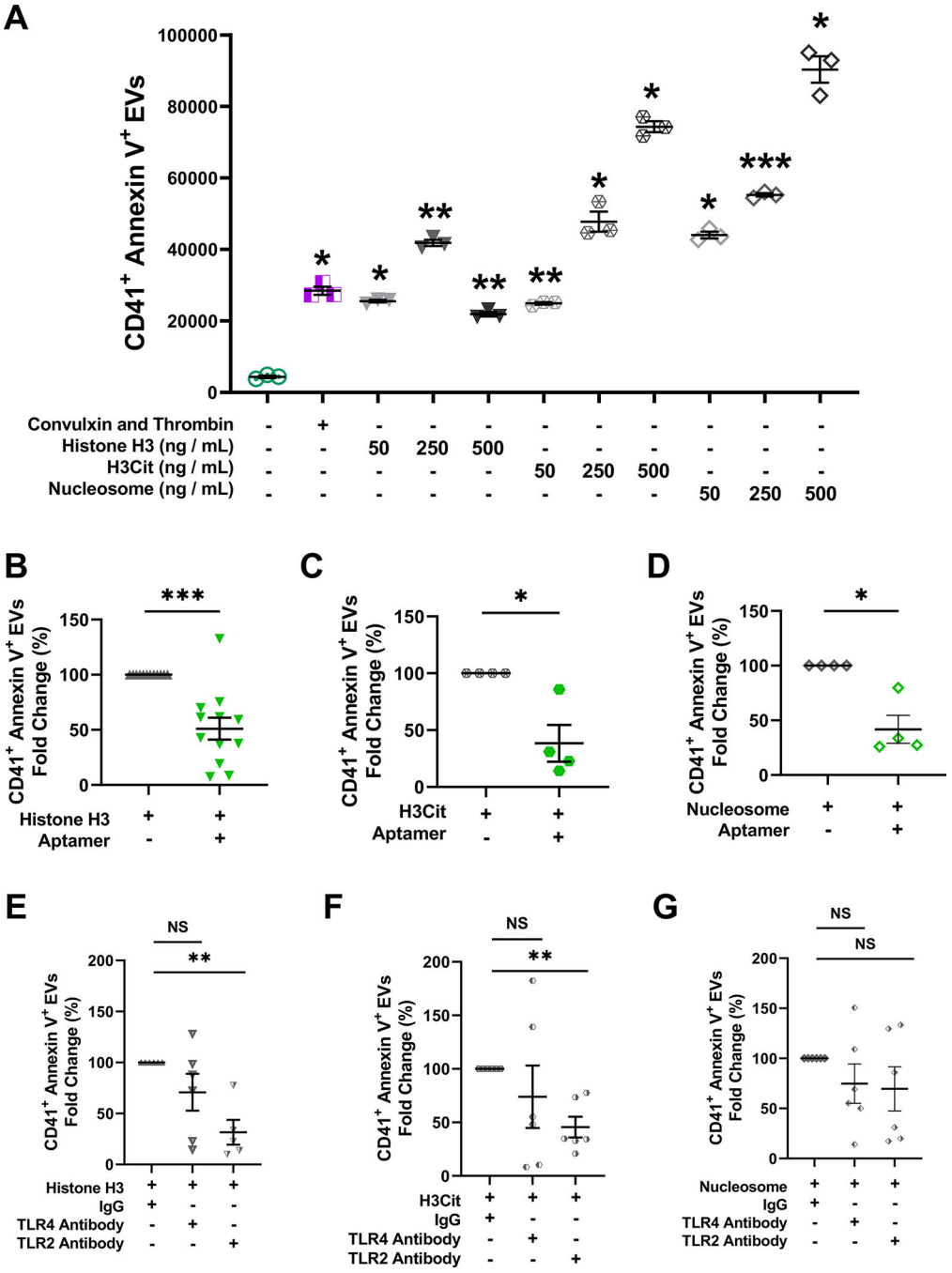

Figure 4. Histone H3, H3Cit and Nucleosomes induce EV production from platelets.

(A) Platelets isolated from healthy subjects were stimulated with buffer (green open circles), thrombin (0.1 units/mL) + convulxin (100 ng/mL) (purple half-filled squares) or varying concentrations of recombinant histone H3 (gray triangles), H3Cit (grey hexagons), or nucleosomes (gray diamonds) for 60 minutes. EVs were collected by ultracentrifugation, stained for CD41 and annexin V binding, and the number of CD41/annexin V-double positive EVs quantitated by flow cytometry. Data were analyzed by one-way ANOVA. **(B-D)** The percent change of platelet-derived CD41/annexin V-double positive EVs formed

in the presence or absence of HBA7 for platelets stimulated with 250 ng/mL **(B)** histone H3 (N = 12), **(C)** H3Cit (N = 4), and **(D**) nucleosomes (N = 4). Data were analyzed by paired t-test. **(E-G)** The percent change of platelet-derived CD41/annexin V-double positive EVs formed in the presence or absence of neutralizing antibodies for TLR2, TLR4, or an IgG control, for platelets stimulated with 250 ng/mL **(E)** histone H3 (N = 6), **(F)** H3Cit (N = 6), and **(G)** nucleosomes (N = 6). Data are presented as mean and SEM. Data were analyzed with a mixed effect one-way ANOVA. * $p < 0.05$, ** $p < 0.01$, *** $p < 0.001$.

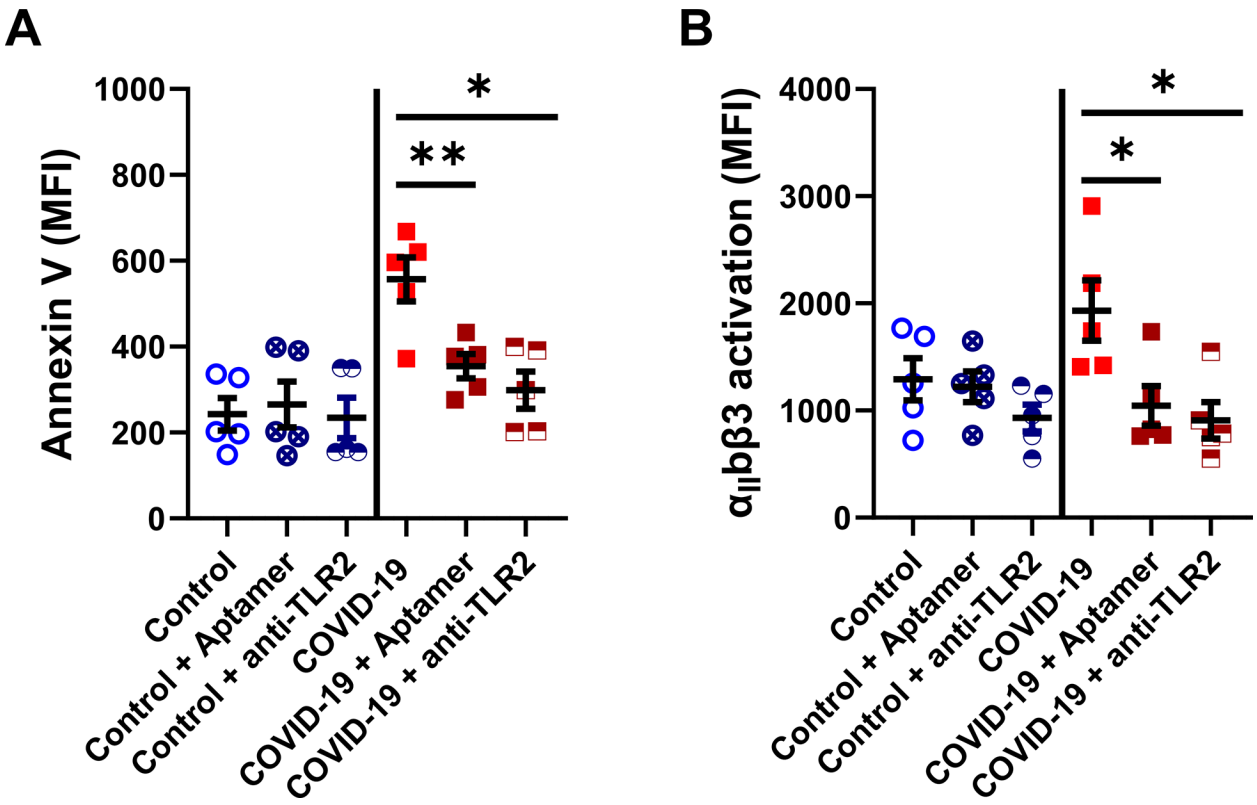

Figure 5. Extracellular histones in COVID-19 plasma promote platelet PS exposure and integrin activation via TLR2.

Washed platelets were isolated from a healthy control subject and stimulated with PPP from either control subjects (N = 5) (blue) or COVID-19 patients (N = 5) (red). PPP were incubated with the histone aptamer HBA7, or anti-TLR2 for 5 min prior to platelet stimulation. Samples were centrifuged, platelet pellets were resuspended in Tyrode buffer, incubated with **(A)** annexin V APC or **(B)** PE conjugated PAC1, samples were fixed, diluted, and analyzed by flowcytometry. Data are presented as mean and SEM and comparisons were made using One way ANOVA with Dunn's multiple comparison within the same cohort.

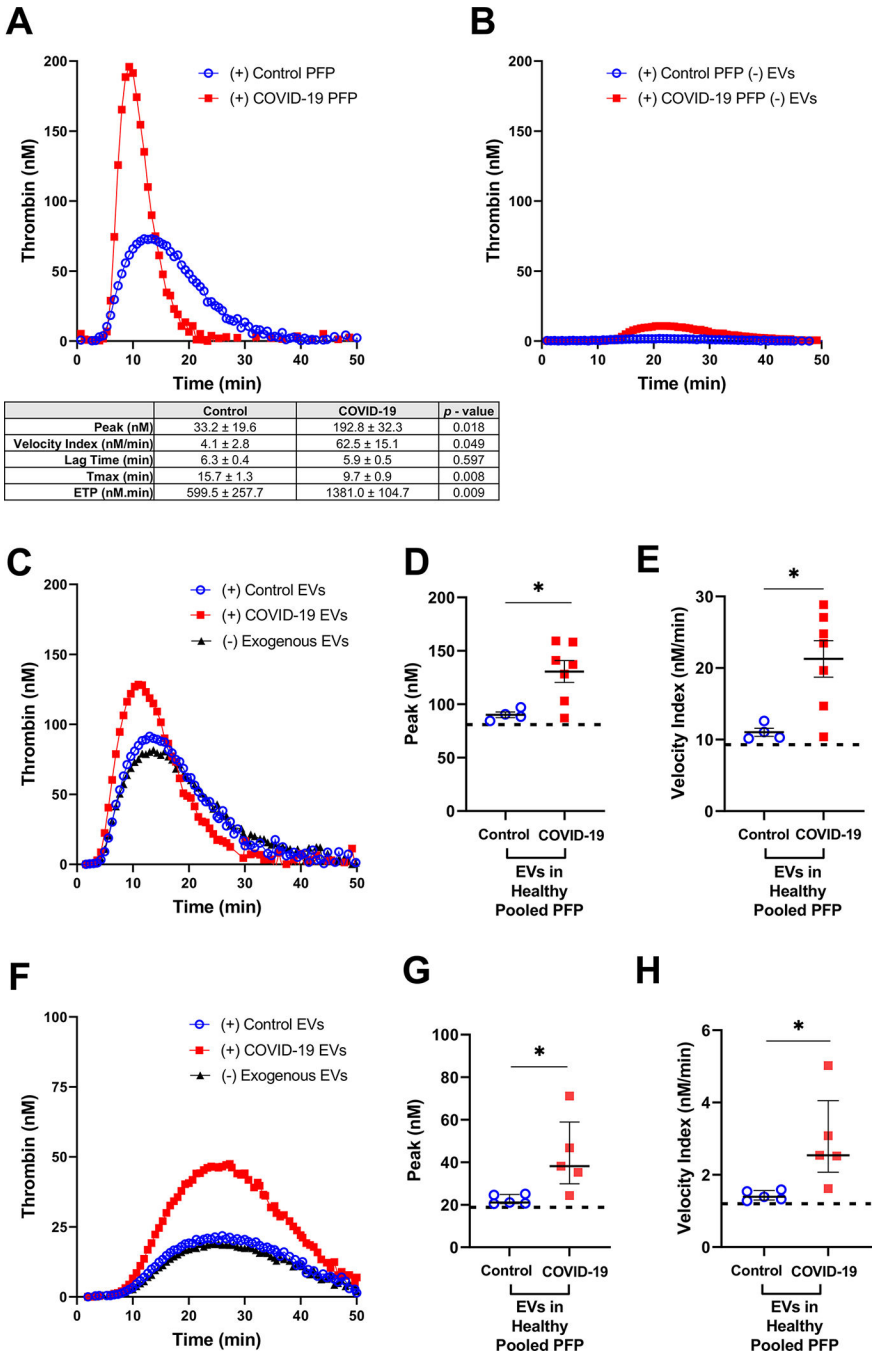

	Control	COVID-19	*p* - value
Peak (nM)	33.2 ± 19.6	192.8 ± 32.3	0.018
Velocity Index (nM/min)	4.1 ± 2.8	62.5 ± 15.1	0.049
Lag Time (min)	6.3 ± 0.4	5.9 ± 0.5	0.597
Tmax (min)	15.7 ± 1.3	9.7 ± 0.9	0.008
ETP (nM.min)	599.5 ± 257.7	1381.0 ± 104.7	0.009

Figure 6. EVs from COVID-19 plasma enhance thrombin generation.

(A) PFP was prepared from healthy control subjects (N = 3) (blue) or COVID-19 patients (N = 8) (red) in the presence of CTI. Thrombin generation was triggered by 1 pM tissue factor (TF) in the absence of exogenous phospholipids. Representative thrombin generation curves and quantitative data are presented. **(B)** EV-free plasma was prepared from controls (N = 4) (blue) or COVID-19 patients (N = 7) (red). Thrombin generation was triggered by 1 pM TF in the absence of exogenous phospholipids and representative thrombin generation curves are presented. **(C)** EV's isolated from control PFP (N = 4) or COVID-19 PFP (N =

7) were added to pooled healthy PFP and thrombin generation was triggered by the addition of 1 pM TF. Representative thrombin generation curves and quantitative data for **(D)** peak thrombin and **(E)** velocity index are presented. **(F)** EVs were isolated from control (N = 5) or COVID-19 (N = 5) PFP by ultracentrifugation and quantitated by flow cytometry. Equal concentrations of EVs (1×10^4 per μL PFP) were added to pooled healthy PFP and thrombin generation was triggered by the addition of 1 pM TF in the presence of CTI. Representative curves thrombin generation curves and quantitative data for **(G)** peak thrombin and **(H)** velocity index is presented. Black triangles, no added EVs; blue circles, EVs from control PFP; red squares, EVs from COVID-19 PFP. Data are presented as mean and SEM for normally distributed data and median and IQR for non-normally distributed data. Comparisons were made using the unpaired t-test (for normally distributed data) or the Mann Whitney test (for non-normally distributed data). $*p < 0.05$.

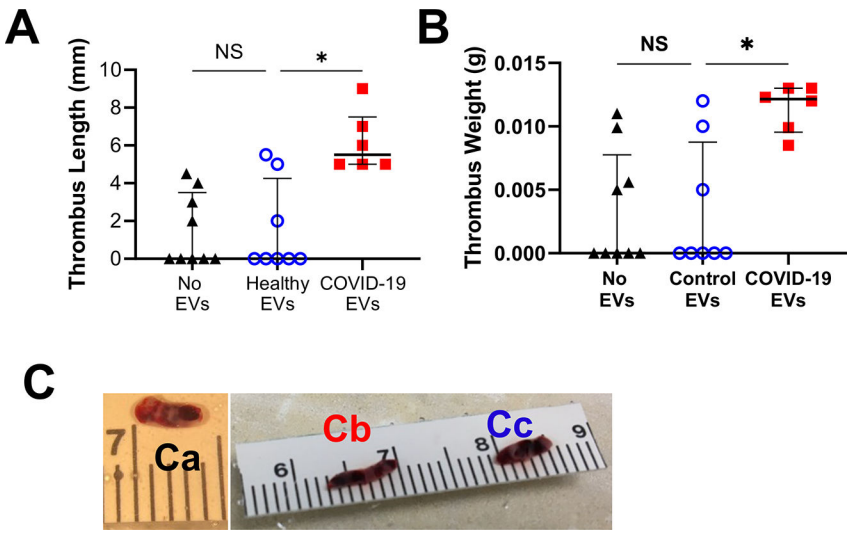

Figure 7. EVs from COVID-19 plasma exacerbate venous thrombosis in mice.

EVs isolated from the plasma of healthy control subjects (blue open circles, N = 8) or COVID-19 patients (red squares, N = 6) were infused retro-orbitally into C57BL6/J mice immediately after venous thrombosis was triggered using a stenosis model of inferior vena cava (IVC) ligation. Thrombi were collected 48 hours after IVC ligation, and the thrombus length **(A)** and weight **(B)** were measured. Black triangles represent the group that were infused with saline (N = 9). **(C)** Representative images of venous thrombus from mice infused with either saline **(Ca)**, or with EVs isolated from COVID-19 or **(Cb)** healthy control subjects **(Cc)**. Data are presented as median and IQR and comparisons were performed using the Kruskal-Wallis test. *$p < 0.05$; NS, not significant.

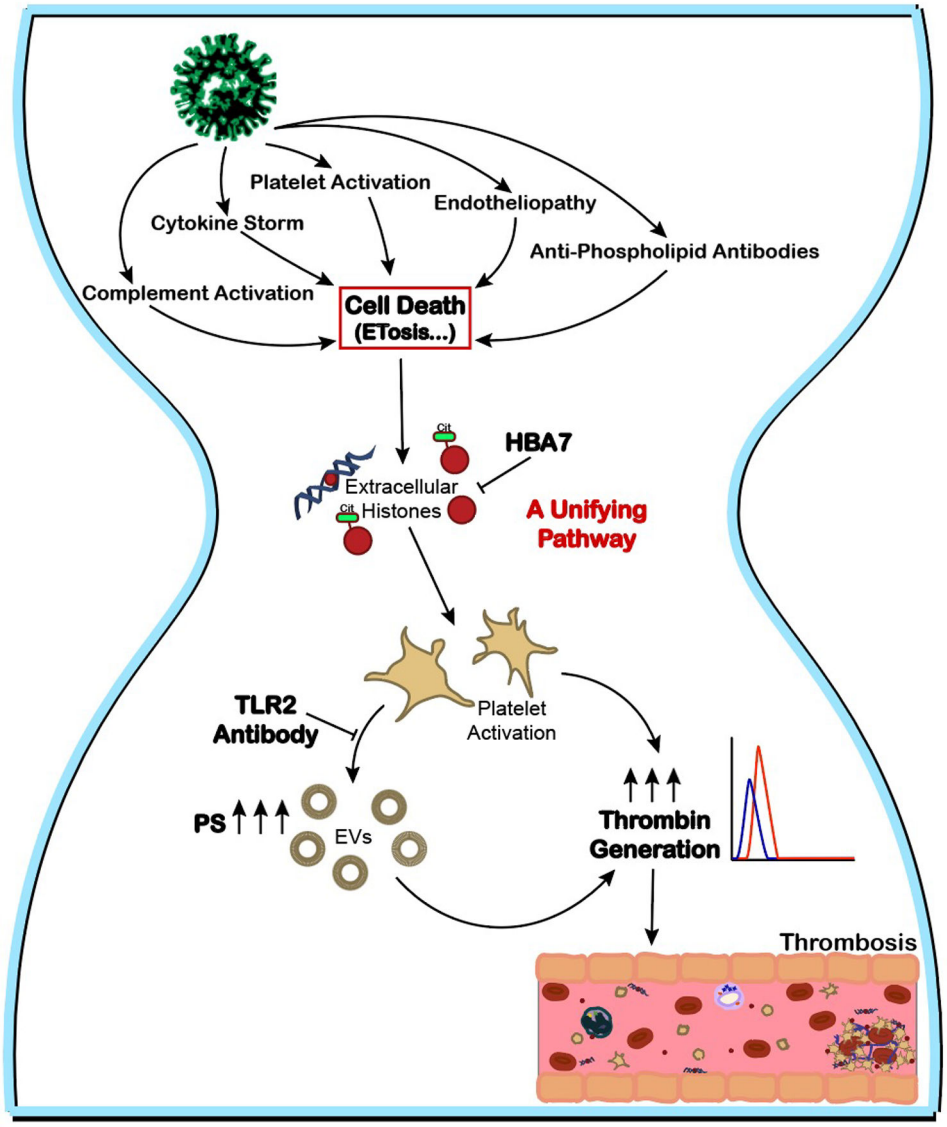

Figure 8. Extracellular histones, a proposed targetable unifying mechanism driving the thrombo-inflammatory state of COVID-19.

Proposed mediators of thrombosis in COVID-19 include complement activation, cytokine storm, platelet activation, endotheliopathy, and antiphospholipid antibodies. All of these processes can induce cell death pathways, including the release of extracellular traps (ETosis), resulting in elevation of extracellular histones. Our data suggest that high levels of extracellular histones in COVID-19 plasma trigger platelet prothrombotic activity via TLR2, resulting in the generation of platelet-derived extracellular vesicles (EVs). The activated platelets and platelet-derived EVs (containing surface exposed phosphatidylserine (PS)) drive thrombin generation and thrombus formation. This unifying prothrombotic pathway can be inhibited by the anti-histone aptamer HBA7. Thus, extracellular histones may represent a targetable unifying mechanism driving the thrombo-inflammatory state of COVID-19.

Table 1.

Baseline characteristics and clinical outcomes

	Healthy/Control Subjects (N = 68)	COVID-19 Patients (N = 103)
Median age - years (range)	38.5 (20-77)	63 (24-85)
Sex - % male	50	53
Median BMI - kg/m^2 (IQR)	25.3 (22.4-28.4)	30.8 (26.9-38.5)
Median laboratory values (IQR)		
White blood cell count (× 10^9/L)	5.2 (4.4-6.2)	9.7 (7.0-12.1)
Neutrophil count (× 10^9/L)	3.1 (2.1-3.7)	7.6 (4.6-10.7)
Lymphocyte count (× 10^9/L)	1.6 (1.1-2.1)	0.9 (0.6-1.3)
Monocyte count (× 10^9/L)	0.4 (0.3-0.6)	0.5 (0.4-0.8)
Platelet count (× 10^9/L)	239 (187-277)	297 (227-380)
Hemoglobin (g/dL)	14.6 (13.8-16.1)	12.2 (11.0-13.6)
Hematocrit (%)	42.8 (40.5-46.9)	37 (34-41)
CRP (mg/dL)	ND *	9.5 (3.9-18.0)
Ferritin (μg/L)	ND *	623 (270-1524)
D-dimer (μg/mL FEU)	ND *	1.5 (0.8-3.9)
Fibrinogen (mg/dL)	ND *	552 (474-659)
Partial thromboplastin time (sec)	ND *	27.0 25.0-30.0)
Prothrombin time (sec)	ND *	11.0 (11.0-12.0)
INR	ND *	1.0 (1.0-1.1)
Clinical outcomes - no. (%)		
30-day mortality	0	18 (17.5)
ICU admission	0	68 (66.0)
Intubation	0	31 (30.1)
Acute kidney injury	0	19 (18.5)
Arterial Thrombosis	0	6 (5.8)
Venous Thrombosis	0	8 (7.8)
Bleeding	0	12 (11.7)
Comorbidities - no. (%)		
Diabetes	0	35 (34.0)
Heart Disease	0	31 (30.1)
Renal Disease	0	10 (9.7)
Lung Disease	0	23 (22.3)
Autoimmune Disorder	0	6 (5.8)
Malignancy	0	10 (9.7)
Chronic Liver Disease	0	0 (0)

* not determined